GeoHazards

MDPI

Article

Megatsunamis Induced by Volcanic Landslides in the Canary Islands: Age of the Tsunami Deposits and Source Landslides

Mercedes Ferrer [1,*], Luis González de Vallejo [2,3], José Madeira [4,5], César Andrade [4,5], Juan C. García-Davalillo [1], Maria da Conceição Freitas [4,5], Joaquín Meco [6], Juan F. Betancort [6], Trinidad Torres [7] and José Eugenio Ortiz [7]

1 Geological Hazards Department, Geological Survey of Spain, Ríos Rosas 23, 28003 Madrid, Spain; jc.garcia@igme.es
2 Geodynamics Department, Complutense University of Madrid, José Antonio Novais 2, 28040 Madrid, Spain; vallejo@ucm.es
3 Geological Hazards Department, Instituto Volcanológico de Canarias, 38320 San Cristóbal de La Laguna, Spain
4 Departament of Geology, Faculdade de Ciências da Universidade de Lisboa, Campo Grande, 1749-016 Lisbon, Portugal; jmadeira@fc.ul.pt (J.M.); candrade@fc.ul.pt (C.A.); cfreitas@fc.ul.pt (M.d.C.F.)
5 Instituto Dom Luiz (IDL), Laboratório Associado, Universidade de Lisboa, Campo Grande, 1749-016 Lisbon, Portugal
6 Biology Department, University of Las Palmas de Gran Canaria, Campus de Tafira, 35017 Las Palmas de Gran Canaria, Spain; joaquinfrancisco.meco@ulpgc.es (J.M.); juanbetancort@gmail.com (J.F.B.)
7 Laboratory of Biomolecular Stratigraphy, Technical University of Madrid, Ríos Rosas 21, 28003 Madrid, Spain; trinidad.torres@upm.es (T.T.); joseeugenio.ortiz@upm.es (J.E.O.)
* Correspondence: m.ferrer@igme.es

Abstract: Evidence for frequent, large landslides on the flanks of the volcanic edifices forming the Canary Islands include outstanding landslide scars and their correlative submarine and subaerial rock and debris avalanche deposits. These landslides involved volumes ranging from tens to hundreds of km^3. The sudden entry of large volumes of rock masses in the sea may have triggered tsunamis capable of affecting the source and neighboring islands, with the resulting huge waves dragging coastal and seabed materials and fauna and redepositing them inland. Here, we present new geological evidence and geochronological data of at least five megatsunamis in Tenerife, Lanzarote, and Gran Canaria, triggered by island flank megalandslides, and occasionally explosive eruptions, during the last 1 million years. The exceptional preservation of the megatsunami deposits and the large area they cover, particularly in Tenerife, provide fundamental data on the number of tsunami events and run-ups, and allow proposals on the sources and age of the tsunamis. Tsunami run-up heights up to 290 m above coeval sea level, some of the highest known on Earth in recent geological times, were estimated based on sedimentological, geomorphological, paleontological, and geochronological data. The research results made it possible to estimate the recurrence of tsunamis in the archipelago during the last hundreds of thousands of years, and to establish relationships between tsunami deposits and the probable triggering island flank landslides.

Keywords: Canary Islands; megatsunami deposits; volcanic megalandslides

Citation: Ferrer, M.; González de Vallejo, L.; Madeira, J.; Andrade, C.; García-Davalillo, J.C.; Freitas, M.d.C.; Meco, J.; Betancort, J.F.; Torres, T.; Ortiz, J.E. Megatsunamis Induced by Volcanic Landslides in the Canary Islands: Age of the Tsunami Deposits and Source Landslides. *GeoHazards* **2021**, *2*, 228–256. https://doi.org/10.3390/geohazards2030013

Academic Editor: Fabio Vittorio De Blasio

Received: 13 June 2021
Accepted: 3 August 2021
Published: 12 August 2021

1. Introduction

Megatsunami waves higher than 40 m have been attributed to voluminous subaerial and submarine landslides (particularly to volcanic islands giant flank landslides), explosive volcanic eruptions, and asteroid impacts. The most outstanding documented examples of megatsunamis are those caused by an earthquake-triggered rock avalanche in Lituya Bay [1], Alaska, 1958, generating the highest wave run-up in recorded history (525 m); the Storegga submarine slide [2,3], Norwegian Sea, 8000 y BP; volcanic island flank megalandslides in Hawaii [4–7], Canary [8–11] and Cabo Verde archipelagos [12–14], throughout

the Pleistocene; the volcanic eruptions and caldera collapses on Santorini [15,16], 3600 y BP and Krakatoa [15,17] in 1883; and the asteroid impacts in both Chicxulub, Yucatán, 65 Ma ago [18,19], and Chesapeake Bay, 35.5 Ma ago [15].

The role of large prehistoric landslides in the geological and morphological evolution of volcanic edifices in oceanic islands has been accepted worldwide in the last few decades. However, until recently, they had not been recognized as responsible for the largest tsunamis on Earth [10–14,20–22], together with those caused by asteroid impacts. This is due to a lack of knowledge on the geomechanical characteristics of these megalandslide processes and their effects, never seen by man, as well as the scarcity of preserved tsunami deposits and the difficulty in their recognition.

Multiple megalandslides occurred during the Pleistocene in the Hawaiian and Canary Islands, where the largest number of events was documented due to pioneering investigations of submarine deposits [23–25]. Several of these landslides involved hundreds of km^3 and removed large portions from the subaerial and submarine flanks of the volcanic edifices. These extreme events and the violent and sudden entry of huge masses of rocks in the sea triggered devastating tsunamis with extreme large run-ups, as deduced from the investigations in the coastal slopes of the Hawaiian Islands, Canary Islands, and Cabo Verde archipelago.

Prehistorical volcanic flank landslide-related tsunami deposits were reported in Hawaii, where tsunamigenic deposits, standing at elevations up to 375 m [4,5] on the coastal slopes of Lanai island, were described as evidence of extreme tsunami run-ups. Later, other tsunami deposits were reported from Lanai [6], from Molokai at 85 m in elevation, extending nearly 2 km inland [26,27], and from the Big Island, at elevations of ~400 m [7]. Tsunami deposits were also recently described on the islands of Santiago and Maio, in the Cabo Verde archipelago, indicating extreme run-up heights of >270 m [14] and >60 m [13], respectively, related to the Fogo volcano flank landslide, some 73 ka ago, and to older Pleistocene flank landslides in Santo Antão island. In the Canary Islands, megatsunami deposits have been described at current elevations of 188 m in Gran Canaria [8] and 132 m in Tenerife [11].

The aim of this paper is to describe the characteristics of the deposits that make them assignable to a megatsunami origin, to establish their age of deposition, and to draw conclusions on their magnitude and triggering mechanisms.

These deposits related to tsunami inundations are located in Teno and Isla Baja areas [10,11] (Tenerife), Piedra Alta (Lanzarote), and the Agaete Valley [8] (Gran Canaria). Despite the rugged morphology and steep cliffs characterizing most coastal areas of the Canaries, the existence of littoral platforms and deeply incised ravines provided the accommodation space for deposition and preservation of the tsunamigenic sediments.

The study presents a revision of the Canary Islands tsunami deposits known so far, compiling and updating existing information, and includes unpublished data on Piedra Alta (Lanzarote), and new information from Agaete (Gran Canaria), Teno and Isla Baja deposits (Tenerife), and the results of more than 140 age determinations of the tsunami deposits obtained by different methods: amino acid racemization in marine shells, thermoluminescence in quartz grains, and U-series analysis in corals. From these new data, the relationship between the tsunami deposits and island flank megalandslides is proposed.

Although unequivocal relationships between landslides and the generation and impact of large tsunamis in the Canary Islands have not been established so far, the identification of tsunami deposits in four coastal sites distributed in three islands of the Canary archipelago, demonstrates the importance and relative high frequency of tsunamis over the last hundreds of thousands of years.

2. Tsunamis Induced by Volcanic Island Flank Megalandslides

No volcanic island flank megalandslides (tens to hundreds of km^3) have occurred in historical times (~5000 y BP). The most recent occurred over 5000 years ago at Réunion island [28], although no deposits were found, testifying the occurrence of a related tsunami.

Another outstanding case (at a much smaller volume) is the most recent flank landslide of the island of Stromboli (Aeolian archipelago), dated at 5–6 ka, and involving a volume of 0.7 to 1.8 km^3 [29,30]. Outcrops of volcanoclastic breccias on the SE flank of the island, extending to an elevation above 120 m above sea level (a.s.l.), are tentatively attributed to a giant tsunami generated by the so-called Sciara del Fuoco landslide [30].

In historical times, the largest volcanic landslides occurred on island arc volcanoes, characterized by rapid failure and tsunami generation, with volumes <3 km^3 (magnitudes significantly smaller than prehistoric events on intraplate volcanic islands, as is the case of Hawaii and the Canary Islands) and a recurrence of ~100 years [31]. The most recent and largest landslide occurred in Ritter island (Papua New Guinea) in 1888 involving a volume ~2.4 km^3 [32], which generated a tsunami with observed maximum run-up heights of 15 m on nearby shores [33]; this event ranks among the most disastrous volcanic events in Papua New Guinea in modern times and caused more than 1500 casualties [34]. At Oshima-Oshima, a small volcanic island in Japan Sea, a landslide of similar volume [35] in 1741 generated a tsunami with maximum wave heights of 10 m, being the most destructive tsunami ever originated in the Japan Sea. Both are the only two large volume (>1 km^3) landslides to have occurred on island volcanoes, according to historical and written records [35].

The only documented historical megatsunami caused by volcanic island flank failure occurred at Mount Unzen (Kyushu island, Japan) in 1792, involving a volume of ~0.34 km^3, producing wave heights up to 25 m in the nearby shoreline [36,37], the worst and largest volcanic disaster in the history of Japan, causing more than 15,000 deaths. The maximum tsunami run-up height reached 55 m [38,39] due to the particular topography of the coasts. Approximately 80 years later, in 1871, the landslide of Mount Ruang (Indonesia) caused a tsunami with waves reaching up to 25 m in height [40].

Recently, in 2018, the failure of the flank of the Anak Krakatau volcano (Indonesia) mobilized a volume of 0.22–0.3 km^3 (one order of magnitude smaller than those of Ritter and Oshima-Oshima), producing a tsunami with run-ups of up to 13 m on the adjacent coasts that caused more than 437 fatalities, the largest death toll from a volcanically induced tsunami since the catastrophic eruption of Krakatau in 1883, and the flank landslide of Ritter Island in 1888 [41].

Thus, even relatively 'small-volume' flank landslides (<1 km^3) have caused destructive tsunamis in historic times, emphasizing the importance of a tsunami hazard associated to this type of event. Landslide tsunamis depend largely on the failure of a submarine portion of the volcanic flank, which may involve much greater volumes of rock than the subaerial portion. In the outstanding cases of Oshima-Oshima and Ritter islands, the landslides were mostly submarine (~2 km^3 in the first case [42], an order of magnitude larger than the subaerial portion), probably due to the low elevation of the islands, with maximum heights of 700 and 780 m a.s.l., respectively. In both cases, there is evidence of the occurrence of a single large landslide, but not of sequential multiple landslides [42,43].

Although not comparable in volume, the typology, failure mechanism, and subaerial and submarine morphological features observed in recent small-scale volcanic island landslides are similar to prehistorical megalandslides in Hawaii or the Canaries, which produced proximal tsunami run-up heights of tens to hundreds of meters on neighboring coastlines [4–8,11].

3. Flank Megalandslides and Tsunami Deposits in the Canary Islands

The Canary Islands (Figure 1) were affected in recent geological times (the last 1 million years) by relatively frequent large flank landslides [44–47]. The destruction of large portions of volcanic edifices, not necessarily associated with explosive eruptions, is part of the geological evolution of the archipelago. Some younger islands (<12 Ma), such as Tenerife, La Palma, and El Hierro, present subaerial and submarine conspicuous geomorphological features, evidencing large recent landslides [48–52]. Intense volcanic activity caused rapid growth of the volcanic edifices in a few million years, reaching thousands of meters a.s.l.,

as in the cases of Tenerife (3715 m) and La Palma (2426 m). The near-limit equilibrium conditions of the flank slopes in these islands together with the low strength of the materials that underlie the emerged portion of the volcanic edifices, added by volcanic processes acting over time, combine to cause flank instability and trigger huge rock mass failures, probably some of the largest on Earth. Such landslides and their sudden and violent entry into the ocean must certainly have triggered tsunamis that struck the coasts of the source and nearby islands. Such huge tsunami waves bear the potential to drag seabed and coastal materials and fauna and to redeposit them inland during extensive and cataclysmic inundations. As a considerable number (at least 10) of large landslides occurred during the last 1 million years in the Canary Islands, megatsunamis should also have been relatively frequent.

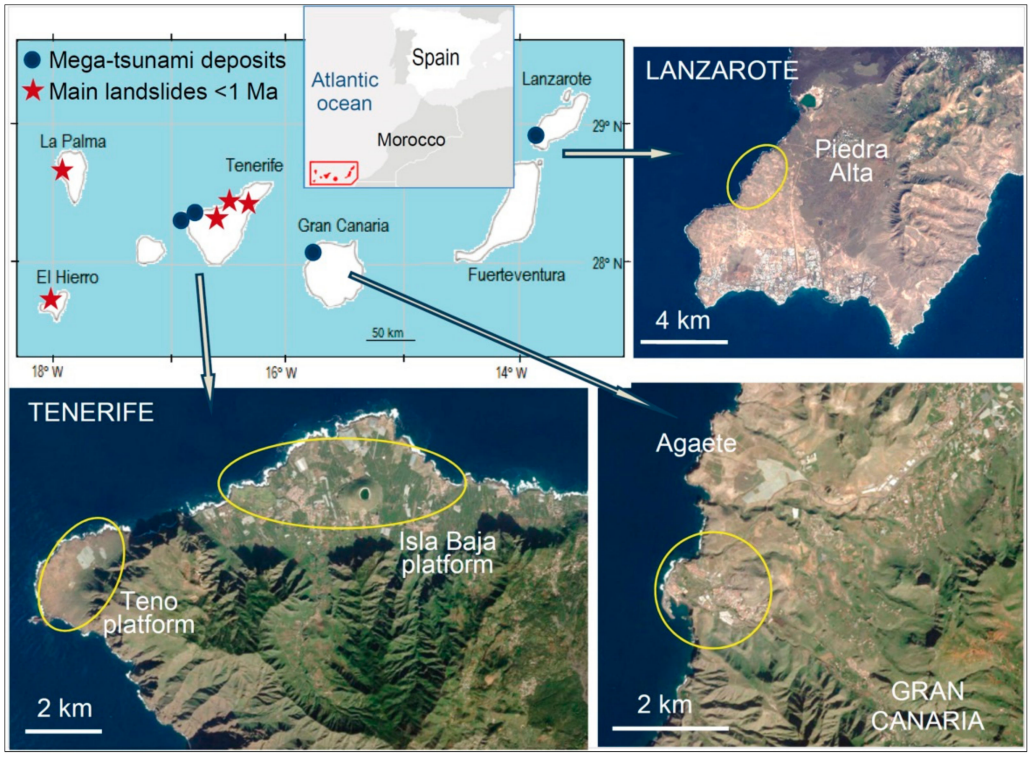

Figure 1. Location of the tsunami deposits and main recent (<1 Ma) megalandslides in Canary Islands. Satellite images with the location of the tsunami deposits at Teno and Isla Baja platforms, Tenerife; Piedra Alta, Lanzarote; and Agaete, Gran Canaria. Google Earth images.

Deposits attributed to megatsunamis were described for the first time in the island of Gran Canaria [8]. Marine deposits on the island of Lanzarote were studied by [53], suggesting a high-energy emplacement mechanism, compatible with a possible tsunami. For the fossiliferous deposits from Teno, in northwest Tenerife, an origin related to a punctual and momentary sea level rise or waves was suggested [54], based on their particular characteristics.

In the GRANDETEN research project, on the causes and mechanisms of the Canary islands megalandslides carried out by the authors of this paper [55–57], the megatsunami deposits of Tenerife and Lanzarote were described and identified as tsunami deposits, and new sites were described in Tenerife and Gran Canaria [9,10,58,59]. The excellent preservation condition of these deposits and their distinctive sedimentological and paleontological features with mixed marine and terrestrial fauna, constitute an exceptional source of information on megatsunami deposits. The characteristics of the sediments indicate a high energy source (they were deposited at tens—even hundreds—of meters above present sea level) and a high speed mechanism, suggesting a relation with the large flank landslides that affected the Canary Islands during the Pleistocene, with giant rock avalanches suddenly entering the sea [10].

Recently, Teno deposits were also described [11] and data on the megatsunami deposits in the Canary Islands were included in review and compilation articles [60,61].

4. Materials and Methods

This work deals with marine conglomerate deposits occurring in three of the Canary Islands, describing the characteristics that undoubtedly allow their attribution to a tsunamigenic origin and their relation to the geologic evolution of the islands, namely the occurrence of large flank landslides during the last 1 million years as a source of the megatsunamis. One key goal was to determine the age of the tsunami deposits to relate them to the flank failure events.

4.1. Field Work

Marine chaotic conglomerate outcrops were analyzed, described, and photographed in the field, and logs and sections were drawn. A detailed map of the tsunami deposits from the Teno platform was produced in the field. Outcrop coordinates were obtained with a hand-held GPS and altitude retrieved from detailed topographic maps and an altimeter. The stratigraphy, texture, and structure of the deposits were recorded, and both sediment and fossiliferous content were sampled. Special attention was paid to the stratigraphic relation with underlying or intercalated formations, which correspond to terrestrial sediments, paleosols, or subaerial volcanic units, and to the nature of contacts between different geologic units. The relation with the local geomorphology was also considered.

4.2. Amino Acid Racemization/Epimerization (AAR) Dating

The AAR method is based on the racemization of amino acids preserved in fossilized biominerals, in this case from *Glycymeris* shells abundant in the tsunamigenic conglomerates. Through time, L-amino acids racemize or epimerize to their D-isomer form; the ratio D/L measures the extent of epimerization.

Glycymeris shells were collected in the four sites to establish their age. The number of samples from each locality is shown in the Supplementary Data. A total of 105 specimens were collected, grouped by locality and collection point, of which 23 were rejected for dating because of contamination by modern amino acids.

For AAR, a hollow diamond drill was used to remove a discoid sample (8 mm in diameter) from an area close to the beak of the shells. Peripheral parts with visible weathering (approximately 20–30%) were removed after chemical etching with 2 N HCl. Afterwards, 10–20 mg of samples were taken.

Amino acid concentrations and D/L values were quantified in the Biomolecular Stratigraphy Laboratory (Madrid, Spain) by high performance liquid chromatography (HPLC) following the sample preparation protocol described in [62]. Samples were injected into an Agilent-1100 HPLC equipped with a fluorescence detector. Excitation and emission wavelengths were programmed at 335 nm and 445 nm, respectively. A Hypersil BDS C18 reverse-phase column (5 μm; 250 × 4 mm i.d.) was used for the separation.

The obtained mean D/L values of the five amino acids (isoleucine, aspartic acid, alanine, valine, and glutamic acid) in *Glycymeris* shells are presented in the Supplementary Data.

4.3. Thermoluminescence Dating (TL)

Samples of calcareous crusts were collected at La Aldea site, in Agaete, on calcrete crusts developed upon the tsunami deposit, with the objective of determining their absolute ages using the thermoluminescence technique and the additive dose method in fine silt-sized quartz particles incorporated in calcrete lining of clasts. The age is determined by means of measuring the accumulated radiation dose, of the time elapsed since sediment containing crystalline minerals was exposed to sunlight. Four samples were collected corresponding to two different calcrete levels, at 74 and 71 m above sea level. The measures and results are presented in the Supplementary Data.

4.4. U-Th Dating of Coral Fragments

Fragments of corals from the tsunami deposits at Teno and Piedra Alta were collected for dating purposes. Subsamples for U-series age determinations were milled from sections of the corals. All samples were (previously) mineralogically and geochemically analyzed, including X-rays, to determine their compositions in the laboratories of the Geological and Mining Institute of Spain, IGME.

Three different groups of analysis were carried out. Two included 6 + 10 samples from Teno and Piedra Alta, respectively, at the laboratories of the Geological Survey of Israel, and a group of 3 samples from Piedra Alta at the laboratories of the Institute of Earth Sciences Jaume Almera, Spanish Research Council (CSIC).

As corals might have suffered diagenetic alteration and opening of the U-Th system, the analysis consisted of analyzing several samples from the same coral; a sequential leaching of the samples was performed to dissolve the bulk aragonitic (or aragonitic–calcitic) coral in weak acid and then redissolved the insoluble residue. For the first group of corals, the measured activity ratios of the individual samples could not provide reliable ages; the same happened for the corals from Teno of the second group. For the corals from Piedra Alta, when looking on the data together, an age of ~120 ka can be assumed, which can be interpreted as the time of diagenesis of the corals by groundwater. The measures and results are presented in the Supplementary Data.

5. Results: Description of the Deposits

Megatsunami deposits that are recognized in several field locations of the Canary Islands share the following common features:

- Sediments correspond to fossiliferous heterometric breccias and conglomerates, both matrix and clast-supported, displaying massive structure and chaotic fabric; clast sizes vary from 1 cm to more than 1 m;
- They are poorly sorted, with a mixture of angular and subrounded clasts, sometimes showing crude normal or reverse grading; frequently two or more layers can be distinguished;
- The sediments present marine or mixed (terrestrial and marine) facies and in all cases overlie terrestrial deposits (paleosols, colluvium, alluvial sediments, eolian sands, subaerial basaltic lava flows), supporting a subaerial emplacement above coeval mean sea level;
- A sharp and erosive character of the unconformity at the base of the tsunamigenic layers;
- The deposits overlie elevate lava platforms or are plastered onto irregular subaerial sculptured slopes, incompatible with long-term marine abrasion related with former sea level high-stands, as would be expected on raised beach deposits;
- A polygenic composition of conglomerates that includes marine-sourced lithic and biogenic elements (rounded beach gravel and boulders, blocks of beachrock, marine bioclastic sand, and fragments or whole marine fossils), subaerial elements (e.g., sub-angular clasts of basaltic nature and terrestrial fossils, including pulmonate gastropods), fragments of unconsolidated materials dragged from the flooded surface, and rip-up clasts of paleosols;
- Marine fossil content decreasing in abundance landwards, where terrestrial fossils (including bird or reptile bones) may occasionally be found mixed with marine shells;
- Marine fossils corresponding to organisms living in a wide depth range, from the shallow littoral to more than 200 m depth (bivalves, gastropods, bryozoans, rhodoliths, corals, and echinoderms); the fossils, frequently broken and lacking surface re-working, were never found in living position;
- Presence of imbricated large and small clasts, indicating seaward and/or landward orientations.

Elevation of the deposits ranges from 2 to nearly 200 m above present-day mean sea level (m.s.l.), providing grounds to estimate the run-up of coeval inundations. Maximum

observed distances of the deposits from the present-day coast up to 1.5 km, with large blocks weighing more than 1.5 ton found higher than 50 m.s.l., and more than 500 m inland.

In the following sections, the specific features of the tsunami deposits in each location are described.

5.1. Teno Lava Platform (Tenerife)

Teno deposits are located on the Teno coastal platform, at the NW corner of Tenerife (Figure 1). The platform corresponds to Pleistocene lava deltas, and offers the flat morphology and space required for deposition and preservation of the materials washed onshore by tsunami waves. These deposits were described in the literature as Pleistocene conglomerates and cemented marine sands, overlying a quaternary marine terrace at 18 m a.s.l. [63]. However, their peculiar sedimentological and compositional characteristics suggest an origin related to punctual and momentary sea level rise or wave action, possibly linked to catastrophic phenomena derived from intense volcanic activity [54].

The Teno fossiliferous detrital sediments (Figure 2) crop out from about 2 m at the coast up to 60 m a.s.l. further inland. They extend over 1.3 km^2, their landward limit lying about 500 m, locally up to 800 m, from the coastline. They are overlain, largely, by a 60–70 cm-thick pedogenized red alluvial fan deposits.

The lava delta and overlying deposits form a poorly dissected surface sloping 3–5% seaward. In places, the original morphology of the lava flows is well preserved and clinckery lava crests crop out from the sedimentary cover. The main stream draining the area is Barranco de Itobal, where the fossiliferous conglomeratic deposits clearly filled an incised and deep alluvial ravine that should have been around 3–4 m deeper than present at the time of tsunami sediment deposition. Subsequent stream re-incision and slope erosion partly removed and truncated the sedimentary infill. The preserved deposits crop out in two sections along both the left and right banks of the creek.

Tsunami sediments present an irregular and patchy distribution (Figure 2), resulting from variable exposure thickness determined by erosion of the alluvial cover. In addition to the common features described above, the Teno deposits show the following characteristics (Figures 3 and 4):

- The deposits range from 0.4 to 0.6 m in thickness at Teno platform, and up to 1.8 m at Barranco de Itobal. They consist of a single or two depositional units showing distinct textural and compositional attributes (Figure 3A–C and Figure 4A–C). However, no marked discontinuity exists between the superposed units, suggesting that the time elapsed between emplacement of the lower and upper units was short;
- The lower unit is composed exclusively of angular and less abundant rounded basaltic clasts from the underlying lava deltas arranged in an open-fabric, largely clast-supported texture with scarce sand matrix (Figures 3C and 4B). The upper unit is composed of finer, but highly heterometric angular fragments of basalt, syenite, phonolite, orange-colored hydrothermally altered lithic clasts, and pumice, embedded in a light-colored ash matrix (Figure 3D). Rounded clasts are absent. In places, the upper unit is less varied and entirely composed of brownish to yellow volcanic ash, containing dispersed angular clasts of fibrous pumice;
- Both units contain fossils of marine and terrestrial origin, including fish bones, vermetid tubes, mollusks, corals, echinoderms, bryozoans, rhodoliths, terrestrial gastropods, and one lizard bone. The marine fossils observed in the breccia include whole shells and fragments of bivalves, with abundant disarticulated valves of *Glycymeris*; fossils are more abundant in the upper unit (Figure 3E–I), and in both units their abundance decreases landwards. In general, thick shells are more commonly found near the base of the breccias, where fossils are also more abundant;
- Both the lower and upper unit display normal grading. The clasts are mostly of small size ($\leq$10 cm), although some elements with long axis reaching 40–50 cm occur dispersed within the sediment. In places, the deposit presents ill-defined lamination roughly parallel to the cross section of the gullies;

- Clasts in the upper unit are embedded in a pyroclastic sand-sized matrix presenting some consolidation. In places, flatter clasts are imbricated in agreement with seaward flow, but less frequent and ill-defined landward flow imbrications were also noted. Largest clasts concentrate closer to the thalweg of the gullies;
- Where the fossiliferous deposits filled deeply incised gullies, as in Barranco de Itobal (Figure 2), the breccias are coarser and the deposits increase in thickness up to 1.8 m. The overall structure suggests rapid emplacement of 4 to 5 stacked depositional units, with a very short time interval between successive depositional pulses; once more, this is confirmed by no marked discontinuities separating the superposed units (Figure 4B). The lower unit (20–40 cm thick) is composed exclusively of angular basalt clasts, with few bioclastic sand matrix; the upper units are similar in composition to those of the Teno platform. At this site, the conglomerates overlie whitish fine and well sorted sands (climbing dunes?) that grade laterally to a pedogenized semi-consolidated brownish sand, which is herein interpreted as representing a paleosol originally developed in eolian sediments (either dune or interdune deposits) (Figure 4C);
- Several large rounded basalt blocks (up to 1.7 m in diameter) stand isolated on the platform; they sit at 40 m a.s.l. and 560 m landward from the present-day coastline and >200 m from the toe of the paleo sea-cliff limiting the lava platform to the east, suggesting inland transport from the coast.

5.2. Isla Baja Lava Platform

Isla Baja area is located in NW Tenerife coast, to the east of Teno platform (Figure 1), and separated by tall coastal cliffs cut in Miocene lavas. As in Teno, an extensive littoral platform developed in relation with subaerial lava flows, provided a low and flat surface that favored deposition and preservation of materials washed inland by tsunami waves. The platform is intensely modified by human activity, mainly for agricultural and urban development, and the tsunami deposit can only be observed at some coastal sites and occasionally further inland. Texture, composition, and depositional architecture of both Teno and Isla Baja deposits are strikingly similar, just as their distribution in elevation and location at the coastal ribbon. These characteristics and the proximity to Teno provide grounds to infer that the deposits of both areas are correlative.

The main outcrop is located in Playa de las Arenas (Figure 5) on the western edge of the platform at 3–4 m a.s.l. and is exposed on a vertical road cut some tens of meters long. The surfaces upon which the conglomerates rest correspond to subaerial lava delta morphologies, slightly modified by subaerial erosion. The main characteristics of the event-deposits are listed below:

- Tsunami deposits are up to 2.5 m-thick and are covered by sandy–clayey colluvium, containing abundant terrestrial fossils (pulmonate gastropods);
- The deposit consists of two stacked conglomeratic layers (Figure 6A,C). Both layers contain marine and terrestrial fossils (bird bones), and are separated by an undulating, locally erosive, surface, without any evidence of a significant time gap;
- The lower layer is at least 2 m thick and highly heterometric, with scarce sandy matrix (Figure 6A). It is composed exclusively of basalt clasts entrained from the underlying lava flows and is characterized by a chaotic fabric. The dominant clast size range is 5 to 10 cm, occasionally reaching up to 1 m; numerous large and elongated blocks standing in vertical position were observed. This layer shows the largest (meter-sized) elements on top, suggesting crude reverse grading. The fossil content includes fragments of marine gastropods and bivalve shells (such as disarticulated valves of *Glycymeris*) and ahermatypic corals;
- The top layer consists of a 1.5 m-thick breccia containing clasts of the same range and lithologies found in the upper layers of the Teno outcrops: basalt, syenite, phonolite, orange-colored hydrothermally altered debris, and pumice. A small number of flat clasts present imbrication indicating seaward flow. Clasts are much finer than in the underlying layer, predominantly in the 1–5 cm size-range, and only occasionally

reaching 20 cm (Figure 6B). The strong contrast in modal particle size observed immediately below and above the surface separating the lower from the upper layers, together with the erosive nature of that surface, highlights the signature of two distinct depositional episodes.

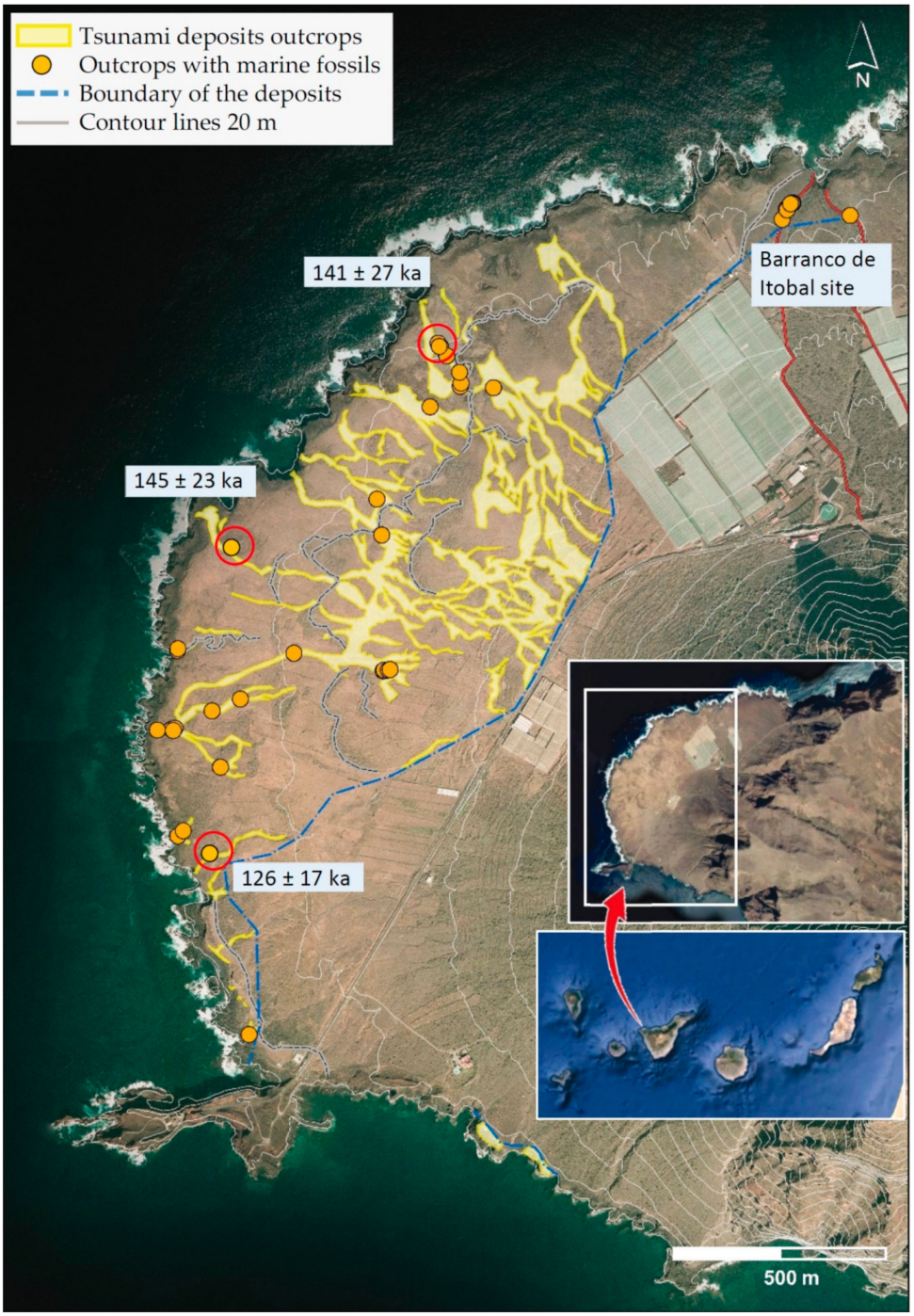

Figure 2. Map of the tsunami deposits overlying the Teno lava platform obtained from a field survey, cropping out the areas where the alluvial cover was removed by erosion. The Barranco de Itobal site is located to the northeast, where the tsunamigenic sediments have maximum thickness. Ages obtained in this study by AAR analysis are included (red circles). PNOA and Google Earth images.

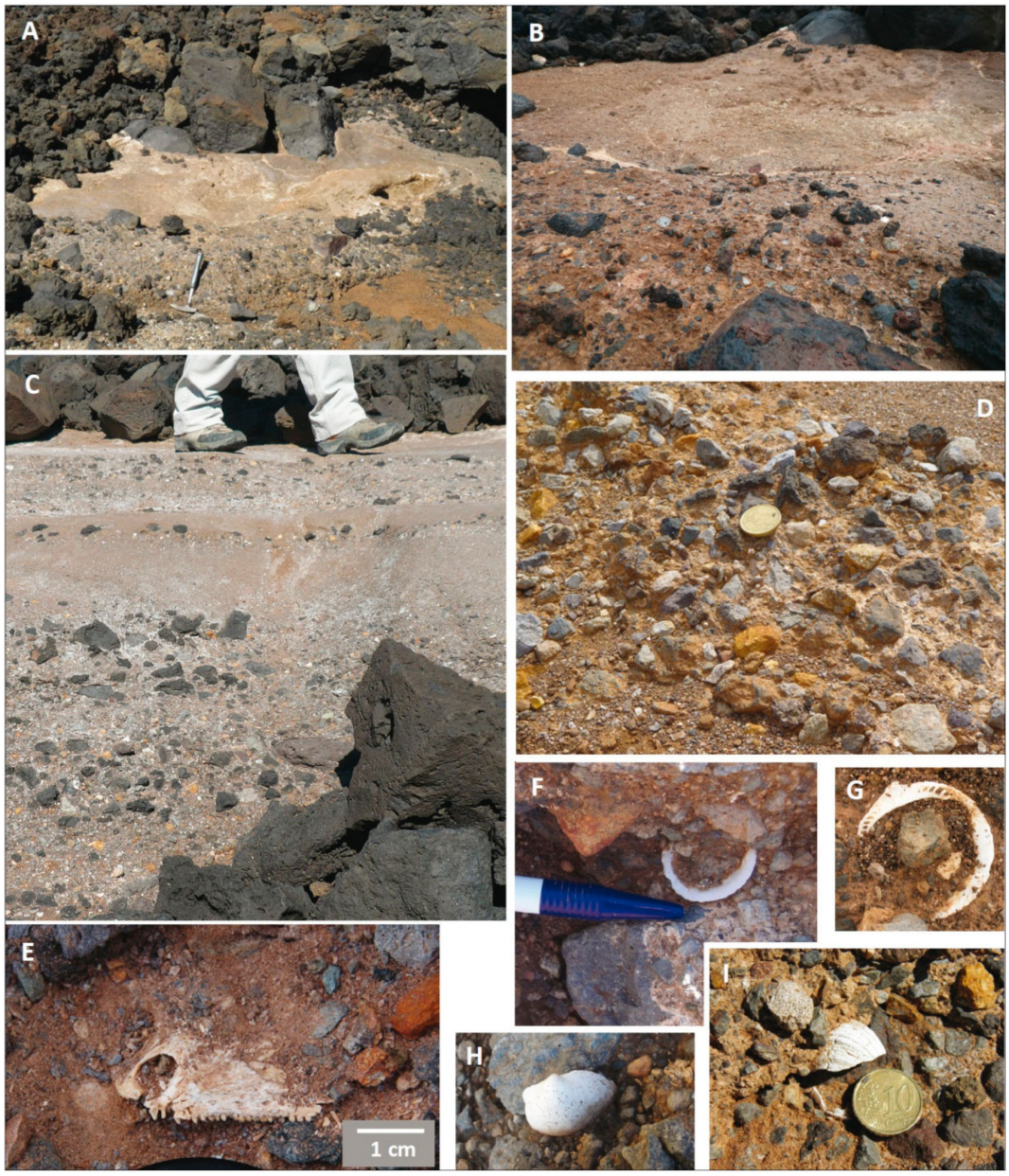

Figure 3. Teno tsunami deposits. (**A**–**C**) Breccia plastered on in situ basaltic lava close to the seaward edge of the Teno platform, showing normal grading and predominance of pumice in its upper section. The breccia contains abundant larger angular basalt (grey) and smaller light-colored heterolithic clasts dispersed in a sand-sized weathered ash matrix. (**D**,**I**) Detail of the heterolithic breccia forming the upper unit of the deposit at Teno platform, with matrix to clast-supported fabric, angularity, and poor sorting of clasts, sand-sized ash matrix, heterolithic composition, and fossiliferous content. (**E**–**I**) Marine fossils incorporated in the tsunami deposit (valves of bivalve shells and a fish skull).

Other outcrops of breccias containing marine fossils, showing compositional characteristics shared with the Playa de las Arenas upper layer, were identified both near the coast (at Lomo de las Campanas and El Rayo sites, at ~2 km and ~3 km, respectively, to the east of Playa de las Arenas outcrop, where the deposits present the same characteristics; Figure 5), and on scattered outcrops further inland. Field observations show that the tsunami deposits extend for about 7 km along the coastline, and reach more than 1.5 km inland where they stand at elevations as high as, or higher than, 150 m a.s.l. At some points on the platform, where soil and vegetation cover has been removed by erosion, or small slopes have been excavated by human action, there are outcrops of the upper heterolithic layer, in some cases containing marine fossils (*Glycymeris* valves). However, except at

Cenizales (Figure 5), neither the complete section nor the basal layer are entirely exposed. At the highest observed points (>150 m), *Glycymeris* shells were not found, and the massive heterolithic deposits exhibits a reworked and re-deposited appearance, indicating a different origin from the subaerial volcanic deposits with similar lithological content present in the area (the so-called *blast* deposit).

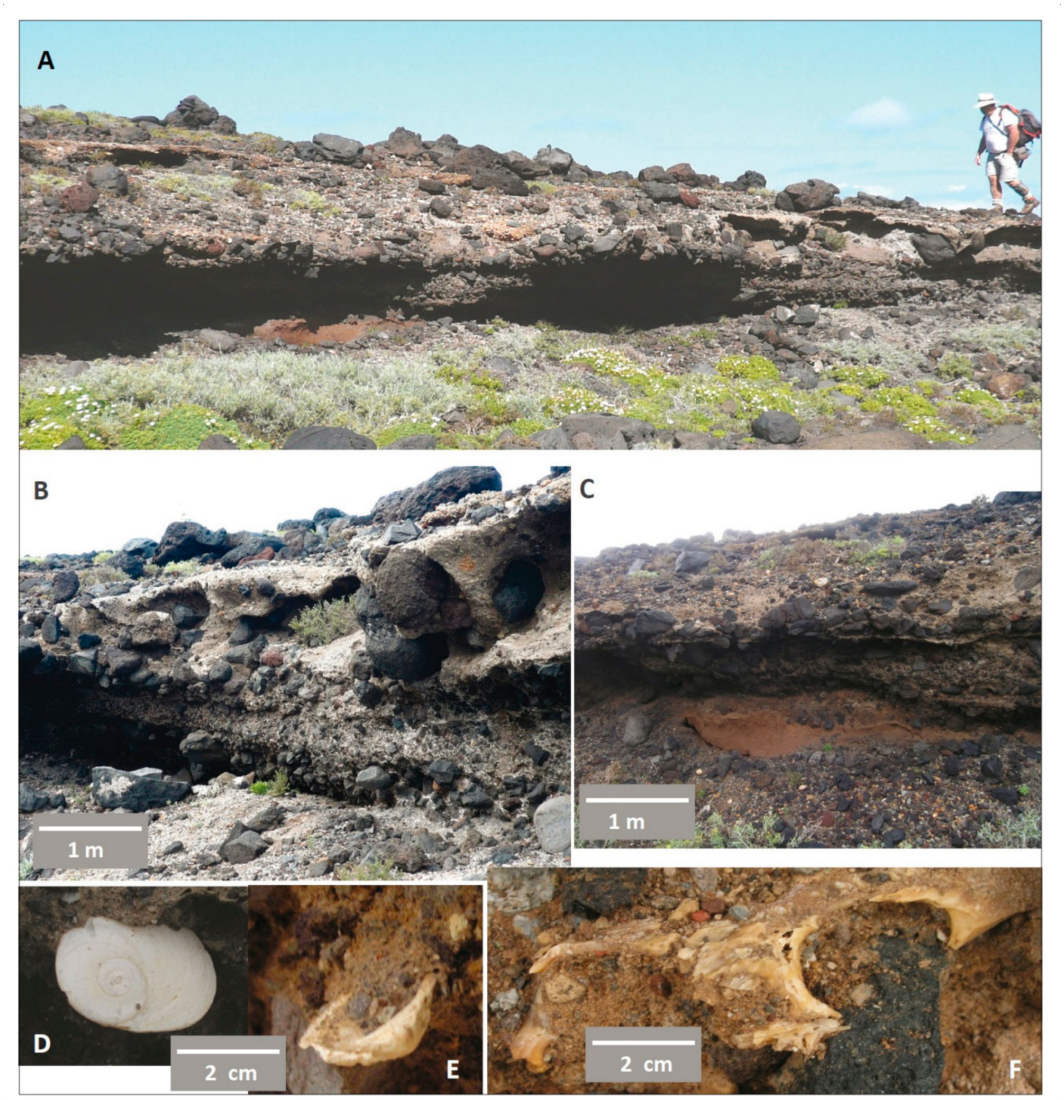

Figure 4. Barranco de Itobal (Teno) deposits. (**A**–**C**) Fossiliferous breccia with multiple depositional layers, up to 1.8 m thick, showing reverse grading; four to five depositional units can be observed (**B**); (**C**) the tsunami conglomerates overlie an Aeolian sand and dune slack deposit on which a brownish sandy paleosol has developed; (**D**–**E**) incorporated fossils of bivalves and gastropods, and (**F**) fish bones.

The most representative and complete inland outcrop is the Cenizales site (28°22′58″ N–16°49′31″ W), located to the east of the platform, at about 50 m a.s.l. and 700 m from the coast (Figure 5). Here, an excavation was carried out for construction materials, allowing the observation of the tsunami deposits, which consist of two layers (Figure 7). Both layers are similar in textural and compositional characteristics to those cropping out at Playa de las Arenas and Barranco de Itobal. The upper 2 m-thick level is a chaotic deposit with centimeter to decimeter-sized heterolithic clasts and fine matrix, containing *Glycymeris* shells (Figure 7A–D). At its base, large (up to 1 m^3) rounded basalt blocks appear surrounded by a consolidated sandy layer (Figure 7E,F). The tsunamigenic sequence is underlain by a pyroclastic subaerial (tuff) deposit.

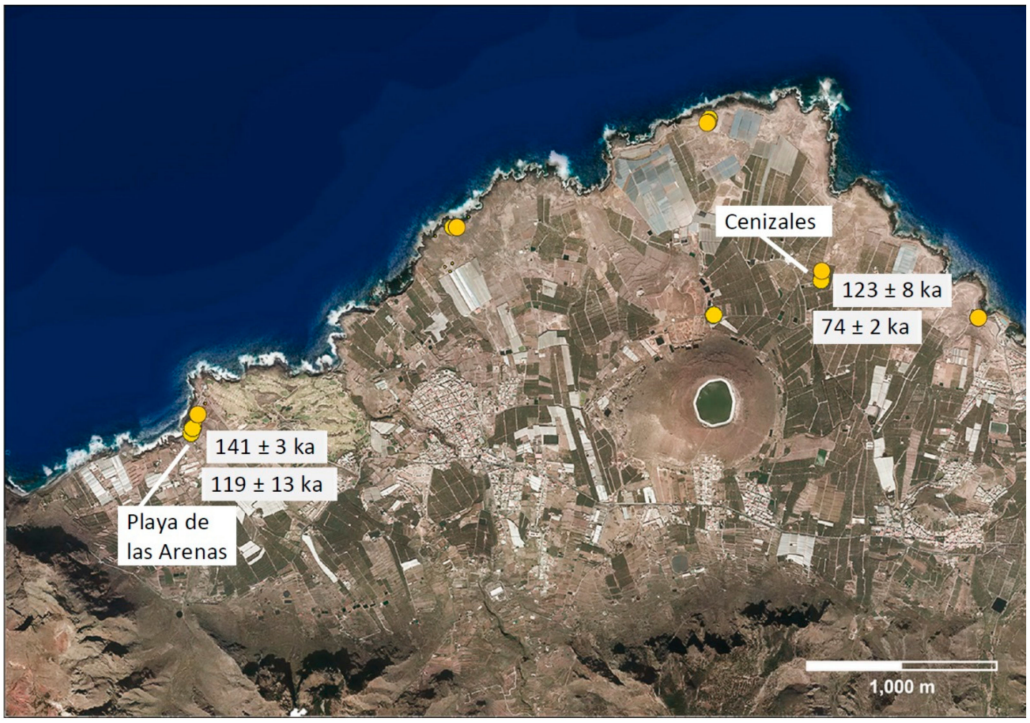

Figure 5. Isla Baja tsunami deposits. The main outcrop is located at Playa de las Arenas. Other outcrops, including Cenizales, the most inland outcrop, are also marked by yellow dots. Ages obtained in this study by AAR analysis are indicated. PNOA image.

5.3. Piedra Alta (Lanzarote)

Tsunami deposits at Piedra Alta, on the SW coast of Lanzarote (Figure 1), stand at 15 to 21 m a.s.l., overlying an elevated coastal platform formed by lava flows. The marine conglomerates were firstly described as a sequence of uplifted marine levels [64], and later assigned to an abrupt and high-energy emplacement mechanism, compatible with a tsunami violently striking this coast during an interglacial period [53]. The deposit extends for several kilometers landward [65], and is partially covered towards the north by a subsequent lava flow. The sediments are well-exposed in several outcrops scattered along the coast for 2.5 km, the longest section being about 200 m (Figure 8A); the deposits can also be observed at the bottom and lateral slopes of some small gullies, up to 15 m inland.

The Piedra Alta's most extensive and representative outcrop is 4 m thick (Figures 8B and 9A,C). Aeolian sand and a red clayey paleosol containing abundant terrestrial fossil fauna, such as insect oothecae and terrestrial gastropods, occur sandwiched between the tsunami deposits and the basement lava flow (Figure 9C,D), indicating subaerial deposition.

The deposits consist of chaotic breccias with angular, frequently broken, clasts of basalt and abundant lithified bioclastic sand matrix. Clast sizes range from 1 cm up to 1.5 m, with blocks larger than 0.5 m predominating in the upper part of the deposit, many of them fractured. Some of the large and flat-shaped blocks are imbricated or oriented, indicating landward flow (Figure 9B); some blocks are covered by a thin layer of marine sand (Figure 9E), indicating a source other than the deposit itself. Fragments from the underlying red colored paleosol (rip-up clasts) are present among the clasts in the lower and coarser layer.

In general, two layers of conglomerates can be clearly distinguished, with marine and terrestrial fossils embedded in a sandy-silty cemented matrix. Between the two layers there is a lenticular one composed of a high proportion of lava blocks and scarce matrix. Fossils are abundant, and mainly occur in the cemented conglomeratic layers. No significant variation in their distribution or content has been observed landwards. A mixture of marine and terrestrial fossils is present, never observed in living position, including a

remarkable abundance of coral fragments of various species. In addition, marine fossils range from deep-sea to infralittoral species. Besides the groups of fossils common to other deposits, the marine fauna also includes brachiopods and crustaceans. Part of the fauna corresponding to the littoral depth-range (corals and bryozoans, Figure 9F,G) is typical of a warm interglacial period and a paleoclimate similar to the present [53]; moreover, some mollusc species in these sediments have never been described in the Canary Islands, but are presently found on the Atlantic coasts of Africa (Senegal, Guinea Gulf), southwards of the Canaries [53].

Figure 6. Playa de las Arenas site (Isla Baja). (**A**,**C**) Outcrops of the fossiliferous breccia with two well differentiated tsunami layers (1,2) contrasting in size and composition of detrital elements, fabric, and abundance of matrix, with crude reverse grading in the lower layer; an earthy colluvium caps the tsunami layers (3). (**B**) Detail of the upper layer with angular poorly sorted clasts of heterolithic composition and marine fossils. (**D**,**E**) Fossils incorporated as clasts in the upper breccia.

5.4. Agaete (Gran Canaria)

Chaotic marine conglomerate deposits, lenticular in shape and up to 3.5 m thick, occur as several isolated and scattered outcrops within the Agaete valley, at the NW of Gran Canaria (Figures 1 and 10). This broad and steep-sloped valley was excavated in Miocene times and its bottom was partially filled by Pleistocene lava flows. Conglomerates crop out from 40 to 188 m a.s.l. and have been described and assigned to a tsunamigenic origin [8].

Figure 7. Tsunami deposits located inland on Isla Baja platform (Cenizales site, see map in Figure 5). (**A**) View of the upper breccia with cm- to dm-sized heterolithic clasts, and (**B**) detail of this layer in the uppermost zone, with smaller heterometric clasts in an ash matrix. (**C**,**D**) Detail of the heterolithic layer containing *Glycymeris* valves among the clasts; (**E**,**F**) large basalt boulders from the lower layer, up to 0.4 m^3, covered by consolidated marine sandstone and remnants of a cemented sandy-ash matrix containing angular basalt clasts and marine shells fragments. Note: the large boulders of the upper part in (**A**) are not in situ.

Agaete tsunami deposits were revisited and provided new data on the sediments [9], including two previously unknown outcrops of tsunamigenic deposits to the existing data set. Furthermore, evidence for the presence of three distinct tsunami inundations was found.

At Llanos de Turman and Berrazales sites (Figure 10), field evidence indicates the presence of two distinct tsunami deposits. The marine conglomerate layers are separated by subaerial deposits (colluvial and fluvial conglomerates with pedogenized tops). The development of the paleosols on these terrestrial sediments indicates that a significant time interval separates the deposition of the tsunamigenic sediments, confirming the presence of two distinct events on those outcrops.

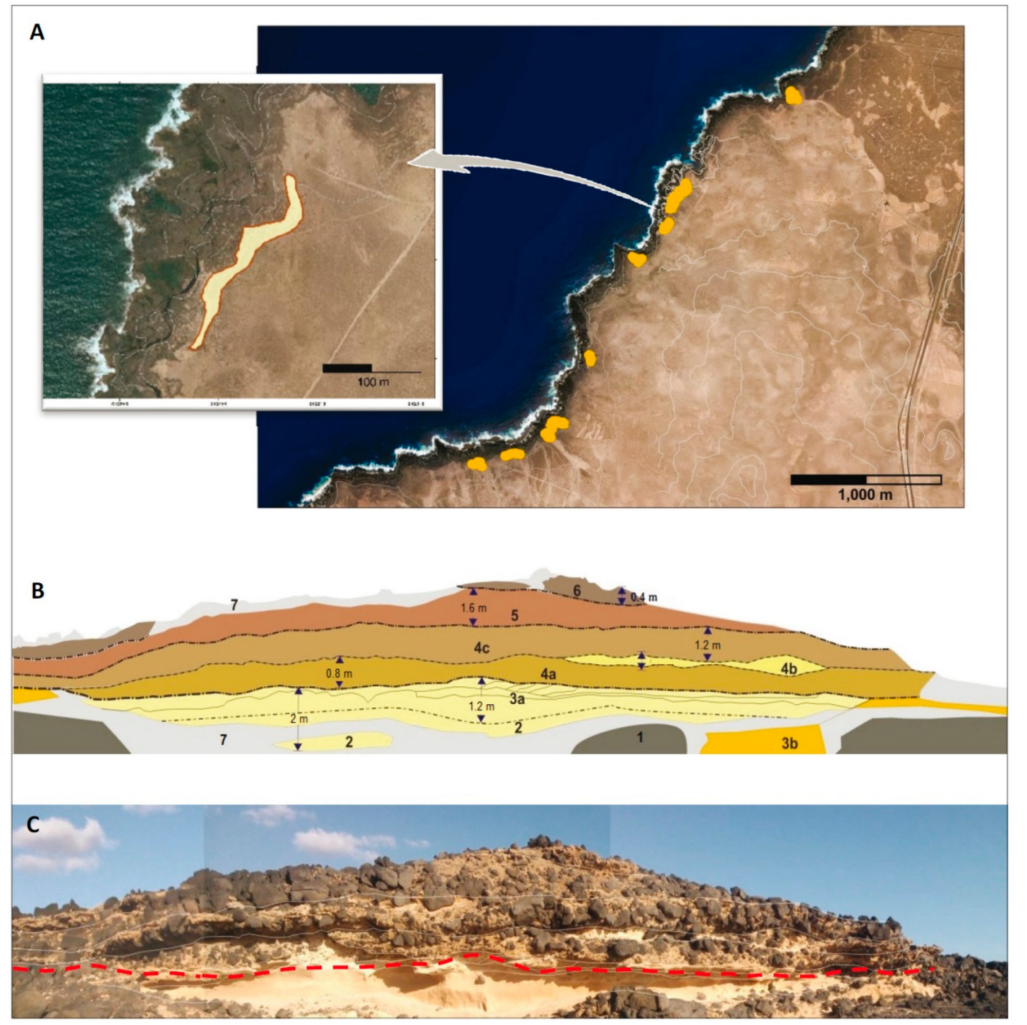

Figure 8. (**A**) Tsunami deposits outcrops scattered along the SW coast of Lanzarote, and location of the main Piedra Alta outcrop. PNOA and Google images. (**B**) Geological cross section of the Piedra Alta deposits in the coastal cliff, at ~20 m a.s.l. 1: underlying lava flow; 2,3: Aeolian sand (paleo dune) and clayey paleosol containing abundant terrestrial fossil fauna, 2 m max.; 4,5,6: tsunami conglomerates showing different layers with erosive contact, cemented sand matrix and basalt angular blocks, terrestrial and marine fossils, 4 m max.; 7: current sandy soil. (**C**) Annotated photograph of the outcrop; length: 30 m (the red line marks the base of the tsunami deposit).

At Llanos de Turman, the structure of the upper marine conglomerate varies laterally. In the center of the outcrop, it is composed of two units: a finer lower unit and a coarser upper unit both reversely graded. Although a well-defined discontinuity separating the two units is absent, there is a sudden textural change marking the transition between the two superposed sedimentary layers highlighted by the deposition of secondary pedogenic carbonates. To the west, the conglomerate is coarser and a third unit is present at the top of the sequence, which is dominantly composed of rounded and finer boulders supported by a sand matrix. The fossil content is abundant including bivalves (*Venus*, *Glycymeris*), gastropods (*Mitra*, *Bolma*), and rhodoliths. Fragments of fossiliferous beachrock are also present. This marine conglomerate covers a torrential deposit whose top is pedogenized. This 50 m-long lenticular torrential deposit is truncated to the east by the overlying tsunami deposit; here the upper marine conglomerate stands directly on top of the lower conglomerate. The contact between the two is marked by carbonate incrustations. The lower deposit is very rich in large (meter-sized) rip-up clasts of paleosol developed on the underlying Pleistocene volcanic sequence (Figure 11F).

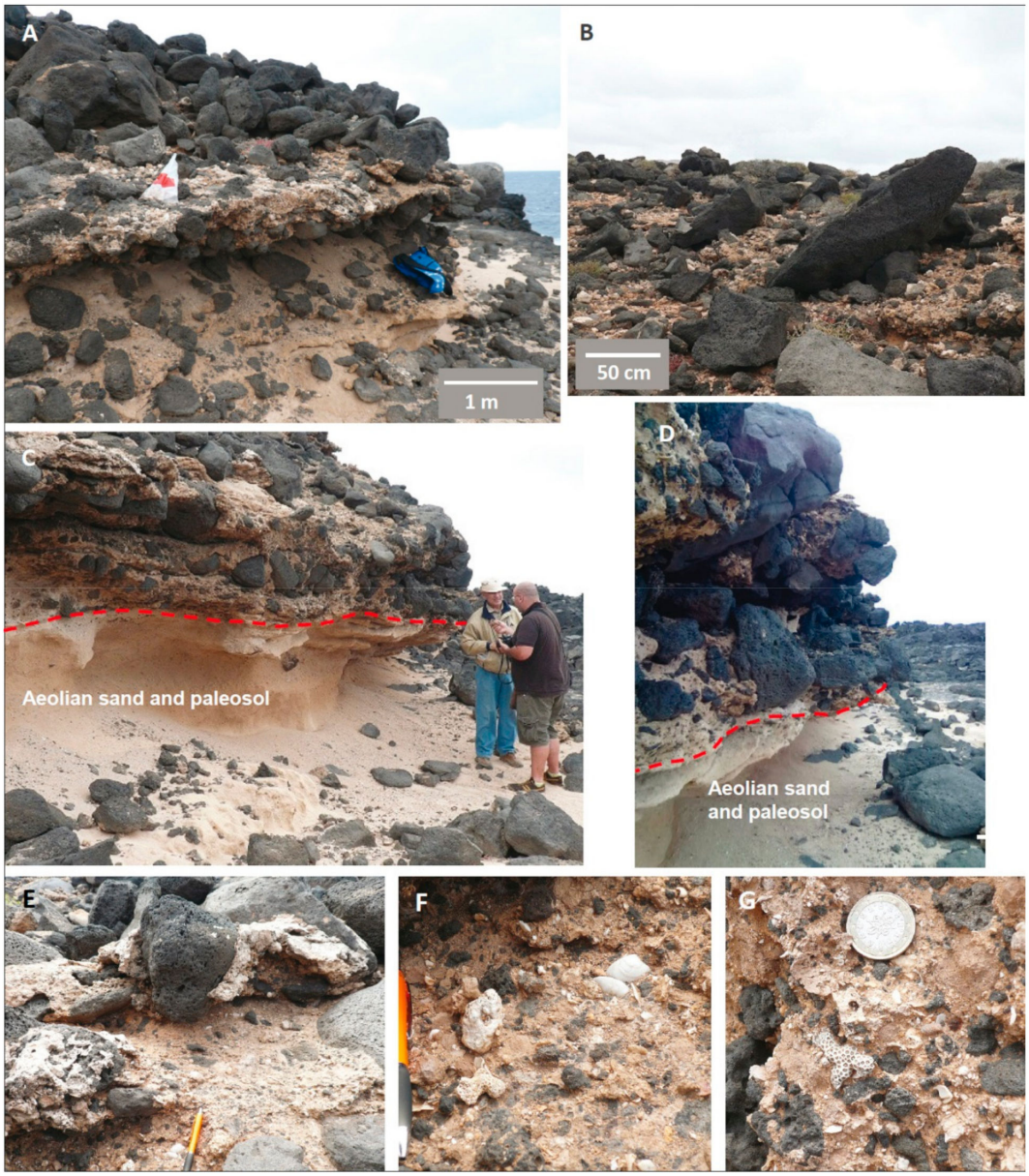

Figure 9. Piedra Alta tsunami deposits. (**A**,**C**) Marine conglomerate (4 m thick max.) overlying dune sands and clayey paleosols containing terrestrial fauna (the red line marks the base of the tsunami deposit); (**B**) imbricated large boulders indicating landward flow, bigger block 1.5 m-long; (**D**) view of a 1.5 m-thick section of the deposit with large angular basalt boulders upwards; (**E**) basalt angular to sub-rounded clasts set in a bioclastic sandstone matrix, with a clast- to matrix-supported texture; (**F**,**G**) marine fossil content: coral fragments and mollusk shells and rhodoliths.

At the Berrazales site, the two marine conglomerates are separated by a sequence of three calcretized colluvial deposits, each presenting a paleosol developed on top. The upper conglomerate contains rare fragmented bivalve shells, while the lower conglomerate displays a mixture of marine fossils and terrestrial pulmonate gastropods (Helicids).

Additionally, an important new outcrop (Figures 10 and 11B,D) was identified on the left bank of the Agaete valley (La Ruina site, 28°05′48″ N–15°41′52″ W) that exposes three stacked fossiliferous tsunamigenic conglomerates separated by alluvial deposits, thus raising to three the minimum number of tsunami events that flooded the Agaete valley. This outcrop is exposed on an artificial cut open for housing construction.

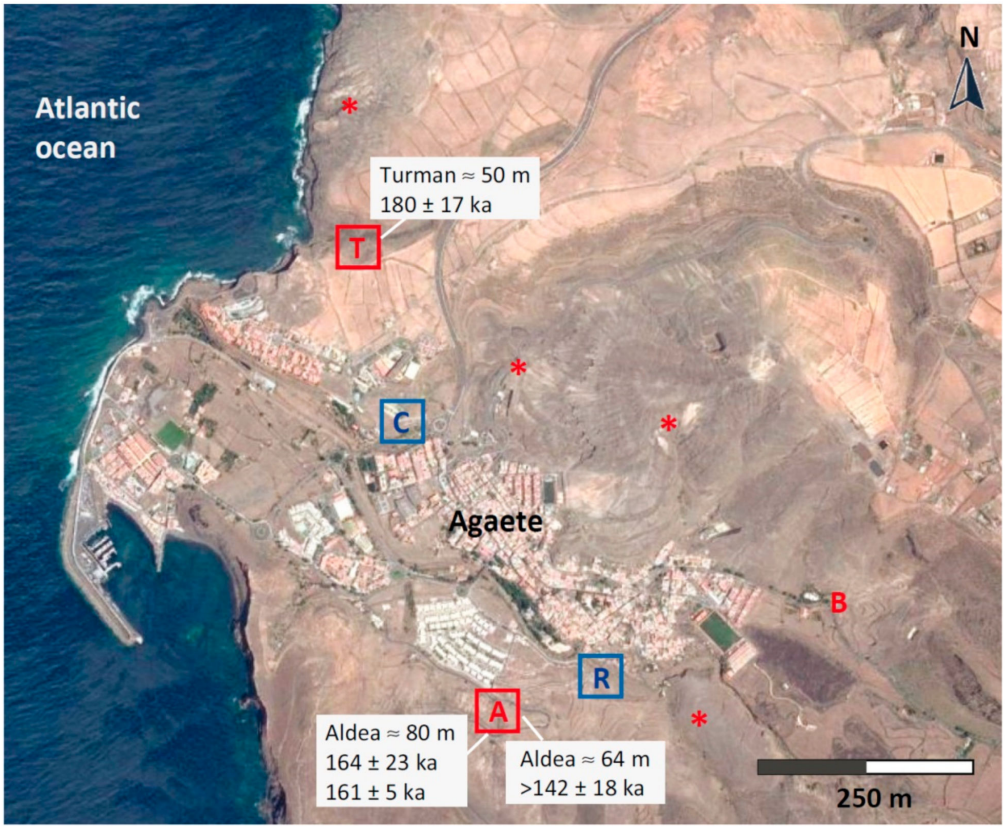

Figure 10. Location of the outcrops of tsunamigenic conglomerates in the area of Agaete (red stars and letters), first described in [8]. Outcrops cited in the text: Llanos de Turman (T); Berrazales (B); La Aldea (A). New outcrops referred in the text (blue): El Cementerio (C) and La Ruina (R). Ages obtained in this study for La Aldea and Llanos de Turman sites are included. Image from Google Earth.

At the La Ruina site, the upper deposit (t3; see Figure 11B) is a 3.2 m-thick chaotic conglomerate presenting reverse grading; the lower part of the deposit displays a clast supported texture, while the upper 2 m are coarser with clasts up to 70 cm in diameter dispersed in a coarse sand matrix (Figure 11D). The clasts are basaltic, and the white sandy matrix is biogenic, although intensely calcretized; fossils are rare and include marine gastropods and bivalve shell fragments. Although there is no evident discontinuity in the deposit, the texture variation may correspond to the two layers observed in the near-by road-cut outcrops of La Aldea (28°05′46″ N–15°41′57″ W; Figure 11A). The outcrop of the upper marine conglomerate, which is certainly correlative of La Aldea sediments, stands at an elevation 10 m lower than the highest 1.8 m-thick road outcrop. It is thicker and much coarser (both in terms of clasts and matrix) and may represent an up-slope (and landwards) fining and thinning of the same depositional unit. This conglomerate stands on an 80 cm-thick pedogenized colluvium deposited on top of another 3.5 m-thick marine chaotic conglomerate (t2; Figure 11B). This layer is finer (clasts 20–50 cm in diameter) and the pedogenized biogenic sand matrix presents a yellowish color. The fossil content is rare and includes fragments of bivalve shells. One distinctive feature of this conglomerate is the presence of abundant rip-up clasts of the friable underlying colluvium (similarly to the lower tsunami deposit of Llanos de Turman). Laterally, this marine conglomerate displays two units: a finer lower unit, covered by a coarser unit (this part of the outcrop is inaccessible). This marine conglomerate rests on a 3.5–4 m-thick sequence of fluvial deposits composed of a thick mudflow (a muddy brownish conglomerate with floating large clasts, presenting a paleosol developed on top) that overlies a lenticular thinly stratified sandy stream flow deposit. Both fluvial deposits cover (and partially erode) a paleosol developed on top of another marine sequence (t1; Figure 11B). This is composed

of two layers: a lower conglomerate with a white sandy matrix containing marine fossils, overlain by a homogeneous sandy layer apparently without fossils. This marine deposit is lenticular in shape and extends horizontally for 12 m.

Figure 11. Tsunami deposits in the Agaete valley: (**A**) general aspect of La Aldea outcrop; the tsunami deposit, overlying a pedogenized colluvium (1), is formed by a basal coarse reverse graded layer (2a) and a finer upper layer (2b), and is covered by a sandy colluvium containing pulmonate gastropods (3); note a downward injected clastic dyke in the center of the photo. (**B**) General view of La Ruina outcrop displaying three superposed tsunami deposits (t1, t2, and t3); the upper tsunami deposits are separated by a brown pedogenized colluvium (col) and the lower tsunami deposit is lenticular and is intercalated within a fluvial sequence (fs) of mudflow and stream-flow deposits; note the presence of a downward injected clastic dyke in the center of t1. (**C**) Aspect of the clast supported texture of the upper layer of the tsunami deposit at La Aldea outcrop. (**D**) Matrix supported texture of t3 tsunami deposit at La Ruina outcrop; the white sandy matrix is intensely calcretized. (**E**) Landwards imbricated flat clasts at La Aldea outcrop. (**F**) Large (~60 cm vertical axis) rip-up clast of red pedogenized basaltic tuff from the underlying volcanic sequence in the lower tsunami deposit at Llanos de Turman. (**G**–**I**) Examples of the fossiliferous content of the lower tsunami deposit at Llanos de Turman outcrop (*Glycymeris*, pecten fragment, and rhodolith). Yellow measuring tape in photos C, D, and E is 20 cm-long.

All three deposits display evidence of erosive bases represented by large rip-up clasts of friable material (deposits t2 and t3; Figure 11B), by erosive truncations of the underlying units (t1 locally truncates t2 and the overlying colluvium), and by downwards injected clastic dikes on their bases (t2 and t3; Figure 11B). One of the dikes is planar and strikes 306°, an azimuth that is probably coincident with the inundation direction, which is certainly controlled by the general trend of the valley. These clastic dikes (also observed on the base of t3 on the road outcrops) can penetrate up to 6 m into the underlying fluvial layers.

The remains of another marine conglomerate outcrop were found on the road access to the Agaete graveyard (El Cementerio site: 28°06′13.2″ N–15°42′11.8″ W, 49 m a.s.l.; Figure 10). This outcrop shares the characteristics of every other tsunami deposit of Agaete and covers a 1.75 Ma-old basaltic lava flow (see below for data on ages of event-deposits and lava flows). The sandy matrix is yellowish, resembling the t2 deposit of La Ruina outcrop, and the deposit contains rare marine fossils (rhodoliths).

6. Discussion

6.1. Age of the Tsunami Deposits

The ages of the different tsunami deposits here described in Tenerife, Gran Canaria, and Lanzarote are discussed below using new data obtained in this study together with previously published ages of lava flows and fossils. Numerical and relative dating of the tsunami deposits was carried out by different methods, summarized in Table 1 and Figure 12. The most consistent ages were obtained by amino acid racemization/epimerization (AAR) and thermoluminescence (TL), in contrast with the U/Th radiometric dating in corals, which strongly depends on the diagenetic evolution and mineral transformation of the fossils. The overall results indicate emplacement of the tsunami deposits during the middle Pleistocene: younger than 168 ka in Teno and Isla Baja; <200 ka in Agaete; and <218 ka in Piedra Alta.

The ages of the lava flows making up the deltas of Teno and Isla Baja in Tenerife, underlying the tsunami deposits, were dated as 178 ± 6 ka and 194 ± 8 ka, respectively [11,66], which provide a maximum age limit for the emplacement of tsunami sediments. AAR performed in *Glycymeris* shells from the fossiliferous conglomerates in Teno yielded ages of 145 ± 23, 141 ± 27 and 126 ± 17 ka that are consistent with the lava flow ages. The ages correspond to three sets of shells collected at different moments with 15, 7, and 11 samples respectively. At Isla Baja, the AAR results from four different localities (with 2, 6, 4, and 6 shell samples) yielded ages within a similar interval, between 141 ± 3 ka and 119 ± 13 ka, except for the age of 74 ± 2 ka from shells collected at Cenizales-2 site, an 'anomalous' value, since another shell from the same area (Cenizales-1 site) provided an alternative age of 123 ± 8 ka. Considering the uncertainties, the ages obtained by AAR in both sites in Tenerife are ≤168 ka. We analyzed two sets of six coral fragments, each from the deposits at Teno by U-series dating method. Unfortunately, no real ages could be obtained, as the corals underwent diagenesis to calcite, influencing the results, so useful slopes on the "property-property" diagrams could not be obtained [67,68].

At Lanzarote, the tsunami deposits from Piedra Alta lie on lava flows with radiometric age of 820 ± 160 ka [69], and are overlain inland by lava flows dated at ~196 ka [53] and 160 ± 20 ka [64]. Based on paleontological and paleoclimatic criteria, they were attributed to Marine Isotope Stages MIS 11 or MIS 13, between ~365 and ~500 ka, based also in a non-decisive U-series age of coral of 481 ± 39 ka [53,70]; later, the deposits have been attributed to MIS 11c, 400–410 ka [65]. Although a wide age range is represented between 820 ka and 160 or 196 ka, both are compatible with new ages of 218 ± 3 ka and 181 ± 27, obtained by AAR in *Glycymeris* shells (two groups of seven samples each) from the tsunami deposit, but these ages are far from the 400–500 ka, to which the paleontological criteria point out (Table 1). As in the case of Teno, we analyzed two sets, 10 fragments of coral each, collected from the deposit at Piedra Alta for U-series. Unfortunately, most of the coral fragments did not provide reliable ages, as they probably correspond to open systems. They show $^{234}U/^{238}U$ isotope ratios that indicate interaction with freshwater, and provide no reliable age information. Only the second set provided ages ranging from 136 ± 6 to

358 ± 48 ka [67,68]. Other additional U-series dating analysis performed for this study provided two radiometric ages of 193 ± 18 ka and >350 ka (Table 1), the former in the same range as those obtained by AAR, but again, far from ages based on paleontological and paleoclimatic criteria. Considering the uncertainties, the ages provided by the numerical methods (AAR and U-series) in Piedra Alta lay between 154 and 221 ka, except for that of >350 ka.

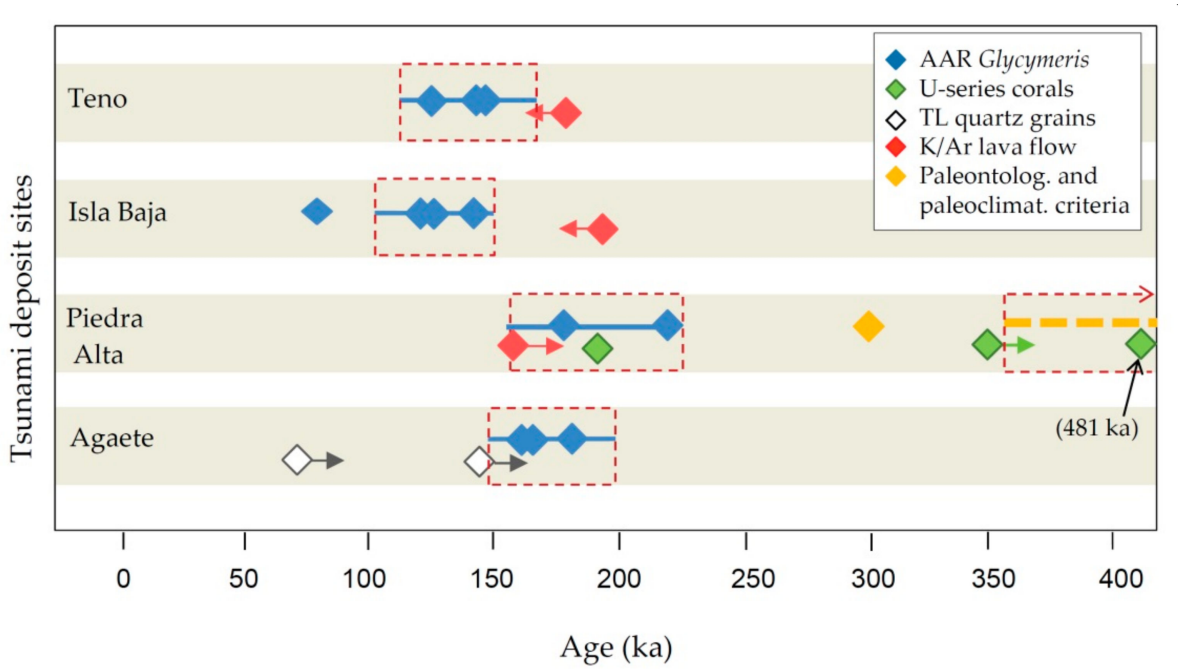

Figure 12. Plot of the age determinations for the tsunami deposits in Tenerife, Lanzarote, and Gran Canaria. K/Ar and paleo-criteria ages from the literature. The dashed red rectangles indicate the most probable ages for the deposits. For Piedra Alta, two alternative age intervals are indicated, although we favor the younger age.

Table 1. Age determinations of the tsunami deposits in the Canary Islands.

Site	This Study (Except *)			Previous Studies	
	AA Racemization	**Thermoluminescence**	**U-Series**	**Lava Flows above/below the Tsunami Deposits (K/Ar)**	**Paleontological and Paleoclimatic Criteria**
Teno Tenerife	145 ± 23 ka 141 ± 27 ka 126 ± 17 ka	-		<178 ± 6 ka [66]	-
Isla Baja Tenerife	141 ± 3 ka 123 ± 8 ka 119 ± 13 ka 74 ± 2 ka	-		<194 ± 8 ka [66]	-
Piedra Alta Lanzarote	218 ± 3 ka 181 ± 27 ka	-	193 ± 16 ka >350 ka 481 ± 39 ka (*)	<820 ± 160 ka [69] >196 ka [53] >160 ± 20 ka [64]	MIS 11 to MIS 13 [53,70] (≈365–500 ka) MIS 11c [65] (400–410 ka)
Agaete (upper deposits) Gran Canaria	180 ± 21 ka 164 ± 23 ka 160 ± 8 ka	>143 ± 19 ka (a) >141 ± 18 ka (a) >62 ± 7 ka (b) >62 ± 8 ka (b)	-	<1.75 Ma [53]	Early Pleistocene [53] (≈1.8 Ma)

(a,b) Data from two different outcrops. The symbols < and > in the K/Ar ages mean that the dated lava flow underlies or overlies the tsunami deposits, respectively. (*) From Ref. [70].

In Gran Canaria, the two younger tsunami deposits cropping out on the Agaete valley rest upon flows from a Pleistocene lava sequence, dated at 1.8 ± 0.03 Ma at Llanos de Turman site [71]. At the El Cementerio site, the marine conglomerates overlie a lava flows dated to 1.75 ± 0.03 Ma [71]. These stratigraphic relations indicate a maximum age bound

of 1.75 Ma for the two younger tsunamis, far from our more reliable AAR results obtained from 17 *Glycymeris* shells contained in three different tsunami deposits at La Aldea and Llanos de Turman (Table 1): 164 ± 23 ka, 160 ± 8 ka and 180 ± 21 ka, ranging between ~140 and ~200 ka when considering the uncertainties. An upper boundary for the age of the younger tsunami deposits from La Aldea site is provided by four ages determined by TL analysis of quartz grains included in two different calcrete crusts developed upon the tsunami deposit, of 143 ± 19 ka and 62 ± 7 ka (Table 1); thus, the higher value is the upper age bound for the tsunami, which is consistent with ages of 140 to 200 ka obtained by AAR analysis. The age data quoted above are from outcrops with elevations between 50 and 80 m a.s.l (La Aldea and Llanos de Turman); for the outcrops at higher elevations in the Agaete valley, no age data are available.

6.2. Sea Level during the Tsunami Events and Estimated Run-Up Elevations

Previous data on the elevation of the tsunami deposits and inundation distance refer to the current sea level. However, variations of sea level during the middle Pleistocene should be accounted for to constrain the run-up heights.

Global sea level curves reconstructed for the last hundreds of thousands of years [72,73] indicate that sea level coeval with the emplacement of the Teno-Isla Baja deposits, assuming an interval 120–170 ka, was in the range of 80 to 120 m below present sea level (b.p.s.l.).

In Piedra Alta, the available data do not allow a reliable age range to be assigned to the tsunami deposits. Two main ranges can be proposed depending on whether the ages obtained by numerical methods (150 to 250 ka) or by paleontological criteria are considered. In the first case, sea level varied between 20 and 100 m b.p.s.l. [72,73]; in the latter case, if a MIS 11 age is considered, then the corresponding interglacial sea level would be 10 to 50 m b.p.s.l. or about 16 to 30 m b.p.s.l. should the deposits be assigned for MIS 13 [65]. In the case of Agaete, sea level at the time of the megatsunamis was most probably between 100 and 80 m b.p.s.l., if an age range of 140–200 ka is considered.

These data indicate that, in all cases, the sea level was tens of meters below present level and, therefore, the run-ups of the tsunami inundations are significantly higher than the highest elevation of the tsunami outcrops, especially in the case of Teno, where more reliable ages were obtained.

Considering that the Canary Islands were stable over the last few millions of years, and have neither undergone neither subsidence nor uplift [74], the minimum run-up elevation (referred to sea level coeval of their emplacement time) reached by the tsunami waves may have been 140 and 230 m for Teno and Isla Baja, respectively, 45 m for Piedra Alta, and 268 m for Agaete. Even considering the occurrence of uplift movements of a few meters in Gran Canaria and Lanzarote in the last hundreds of thousands of years [70], this would virtually have no influence on the run-up heights indicated above. In the north of Tenerife, in addition to the lack of uplift movements [75], the tsunami deposits occur from the coastline, thus indicating that the position of coeval sea level would have been lower than present.

6.3. Tsunami Sources

The identification of at least four noteworthy middle-Pleistocene tsunami deposits on three islands of the Canary Archipelago and the occurrence of several tsunami deposits on the same site, corresponding to different events (at least three distinct tsunamis in Agaete), highlight the relatively high frequency of tsunamis generated by the abrupt entry of very large volumes of rock masses into the sea. Such huge mass movements correspond to large-scale volcanic flank landslides, capable of generating giant waves that would have struck the coasts of both the source and nearby islands.

At least 10 large landslides occurred over the last 1 million years in the Canary Islands, with those of Icod, La Orotava, Güímar, and Micheque in Tenerife (the latter has no morphological features on the surface, as the valley was completely filled in by successive

lava flows), Cumbre Nueva (La Palma) and El Golfo (El Hierro) involving outstanding volumes, in the order of tens to hundreds of km^3 (Figures 1 and 13). None, however, has taken place on the remaining islands of the archipelago during this period.

The relationship between the tsunami deposits here described and the most recent landslides on the islands of La Palma and El Hierro, the westernmost islands of the archipelago, can be practically ruled out since they are far apart, at opposite ends of the archipelago. On La Palma, the last megalandslide, named Cumbre Nueva, occurred 540–560 ka ago [49,77,78]. On El Hierro, four to five megalandslides have occurred during the last 200 ka [49], including the most recent of the Canary islands, in the El Golfo area, where at least two superimposed large flank failures have been identified by subaerial and submarine morphological evidence [51,79]. They have been assigned controversial ages, around 15–20 ka and 130–136 ka [49,50,78], or between 39 ka and 87 ka [80].

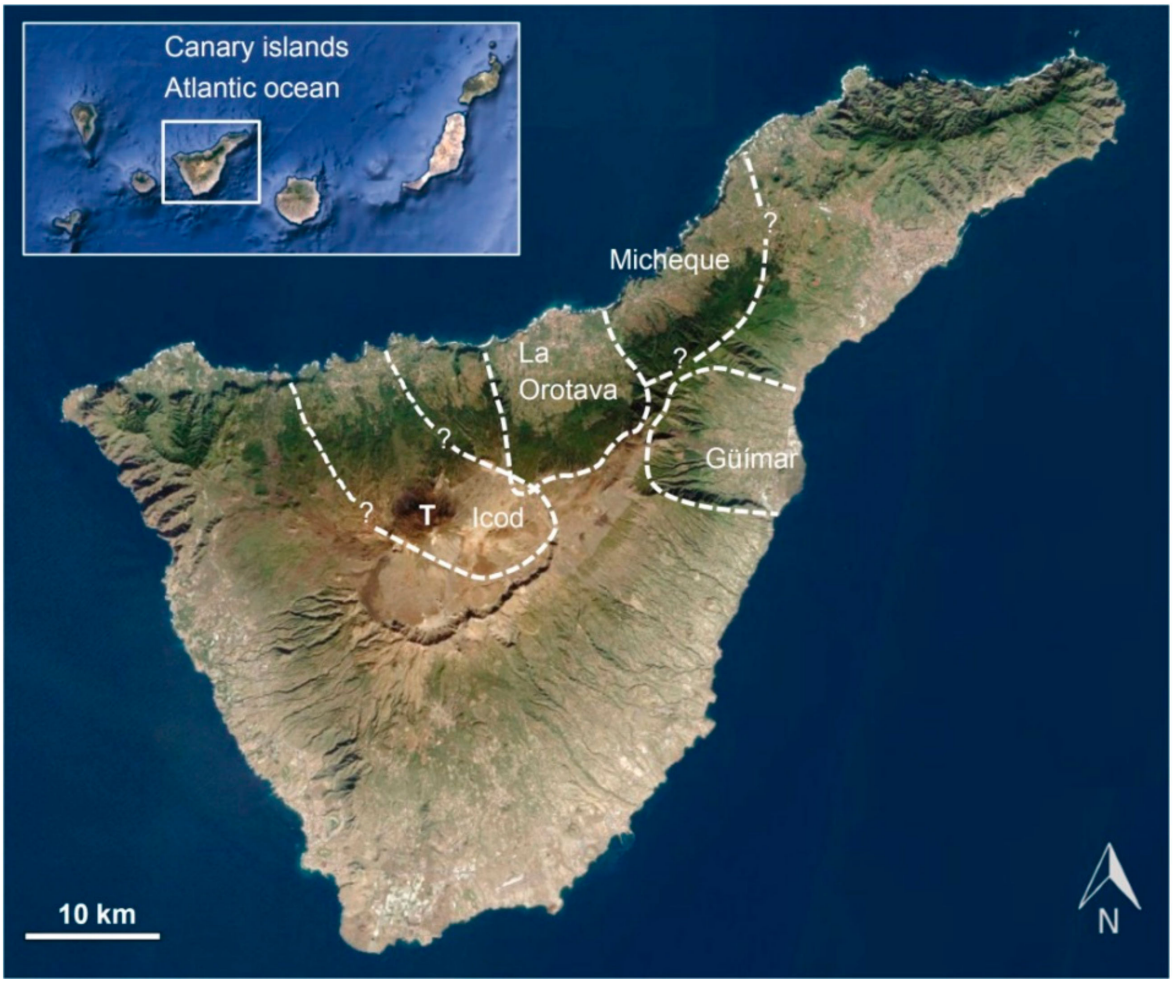

Figure 13. Schematic representation of the most recent landslides in Tenerife: Icod, La Orotava, Guímar, and Micheque or Acentejo, the latter without morphological features on surface. T: Teide volcano (3715 m). Limits of Micheque landslide from [76]. Basemap: GRAFCAN.

The main argument ruling out the La Palma and El Hierro landslides as a source for the identified tsunamis is that those landslides were directed towards the north and west, in opposite directions to the location of the islands where the tsunami deposits have been identified. Another consideration is wave attenuation imposed by distance between the potential tsunami sources and the impacted areas, even though tsunamis can have extremely high initial wave heights of hundreds of meters at the source point and nearby coasts.

The Icod landslide, in Tenerife island, at around 165–175 ka (see Table 2), is related to a large phonolitic explosive eruption (blast) triggered in response to the sudden decompression of the magma chamber caused by the northern flank landslide of the Las Cañadas edifice [81–83]. The resulting massive explosive deposits, rich in heterolithic angular fragments, are distributed throughout the northwest area of the island, presenting a thickness of more than 3 m at the Isla Baja platform.

The data presented above and field observations in Teno and Isla Baja (Tenerife) suggest that the two well-differentiated stacked tsunami units are related to the Icod massive landslide and the ensuing volcanic blast, both events separated by an extremely short time interval (a few minutes?). The first inundation pulse was triggered by the large-scale flank landslide that preceded the blast, and was followed by a second pulse (each pulse consisting of one or several large waves) produced by the rapid entry of voluminous pyroclastic flows into the sea. This chronology and rapid succession of events is imprinted in the sedimentary record at Teno and Isla Baja (Figures 4B and 6A), where the lowermost tsunami deposits contain angular basalt clasts from the lava deltas representing an early inundation of the lava platforms during the initial pulse. This inundation also transported marine coastal sand and shells landward, mixing them with terrestrial material (angular clasts, bones of pulmonate organisms, such as lizards; Figure 3E) collected from the subaerial portion of the lava delta. The mixture of terrestrial fossils with marine shells is to be expected in a landward transport context. The mixed sedimentary load would then have been released suddenly as the water flow reduced intensity, just before or during withdraw to the sea. Landward-dipping imbricated clasts occasionally found in the deposits, testify deposition during out-wash and the extremely chaotic nature of the deposits in terms of particle size, sorting, and directional properties is compatible with a single, extreme-energy marine-borne inundation event. It is noteworthy that in the tsunami deposits at Isla Baja, just at the western boundary of the Icod landslide, and in the nearby outcrop of Barranco de Itobal, in Teno platform, a greater development of the lower layer with large basalt boulders occurs, while on the large extent of the Teno lava platform, farther away and located outside the direct impact of the waves caused by the landslide, this layer shows smaller thickness and size of the basalt clasts.

Table 2. Age of the most recent (last million years) landslides in Tenerife ([52] and references therein).

Landslide	Dated Deposits and Inferred Age for the Landslides from the Literature			Ages [52]
	Volcanic Deposits	Age Range	Representative Average Age	
Icod	Subaerial volcanic deposits affected by or related to the landslide, and valley-infilling deposits	161–198 ka	~165–175 ka [a] 160–180 ka [b]	–
	Distal turbidite deposits from the landslide	160–200 ka		
La Orotava	Subaerial deposits of the landslide scarps, and valley-infilling deposits	540–566 ka	~560 ka	~500 ka ~530 ka ~560 ka
	Distal turbidite deposits from the landslide	500–540 ka	~535 ka	
Güímar	Subaerial deposits of the landslide scarps, and valley-infilling deposits	830–860 ka	~830 ka [c] 830–840 ka [a]	~830 ka 1 Ma?
	Distal turbidite deposits from the landslide	830–850 ka		

[a] Considering the most representative data of both subaerial deposits and submarine sediments. [b] Considering only the ages of the deposits directly related to/affected by the landslide: upper scarp layers and early valley in-filling deposits. [c] Considering the most representative data from subaerial deposits. Modified from [52].

The second inundation pulse, which probably occurred within a very short time-interval after the first wave, essentially transported and delivered lithic and juvenile fragments (pumice and ash) to the coast. These materials were sourced from the pyroclastic

flow violently entering the sea and were eventually mixed with the remaining marine shells and sediments of the coastal fringe that had been previously swept and depleted of coastal sediment during the earlier inundation phase (Figure 3D,I; Figure 4B; Figure 6B). The second pulse may have encompassed several waves. Evidence for this is the presence of three to five layers containing material from the pyroclastic flow found at the Teno platform, though it is not clear if every layer represents an inrush event. The composition of the deposits shows their relation to the volcanic blast event, and the absence of internal structure and the massive chaotic character of each sedimentary unit are consistent with high-energy, short-lived transport. The inundation of the subaerial portion of the lava deltas facilitated the mixture of terrestrial (e.g., *Helicidae* shells and vertebrates bone fragments) with marine fossils.

The age obtained for the Teno and Isla Baja deposits through AAR is $\leq$168 ka, a result within the same age range attributed to the Icod flank landslide (165–175 ka ago) and the associated explosive eruption [52].

The thickness of the marine coarse-detrital tsunami deposits decreases very rapidly westwards, along some 9 km of coast. It exceeds 3.5 m at Playa de las Arenas (Isla Baja), decreases to about 1.8 m thick at Barranco de Itobal, and is just 0.4–0.6 m at Teno platform. This can be interpreted as a very fast lateral (alongshore) westward decrease in amplitude of the tsunami waves produced by a source located further east on the same coast. The Icod landslide and pyroclastic flow(s) were probably directed towards the north, focusing most energy on that direction, with a rapid loss of wave energy occurring along the coast and away from the source point.

At Piedra Alta, the ages provided by the numerical methods (AAR and U-series) suggest an age range of 154 to 221 ka, considering the uncertainties, while from biogeographical/paleoclimatic criteria an age of 365–500 ka has been assigned [53,65]. A plausible correlation can be proposed with two of the large landslides on Tenerife, the nearest island and most likely source of the tsunamigenic landslide. Considering the age of the Tenerife landslides, the Icod landslide (165–175 ka) is compatible with the AAR age interval, while one of the landslides that probably occurred in the La Orotava valley at ~500 ka (Table 2), is within the higher age range proposed from biogeographic/paleoclimatic criteria. Since an uncertainty range is not provided for the 196 ka age of the post-tsunami lavas [53], it is not possible to assess the consistency with the age of the Icod landslide; however, the alternative age of 160 $\pm$ 20 ka for the same lavas [64] does supports this correlation. If either the Icod or La Orotava landslides, which affected the northern flanks of Tenerife, were the source of the Piedra Alta tsunami, the distance between the two islands would explain the 'low' run-up height ($\geq$45 m, a much lower height than the run-ups observed at the coasts of north Tenerife) observed in Lanzarote.

The tsunami deposits that occur in Agaete had previously been attributed to the Guimar landslide, based upon their location in front of the landslide scar on the opposite coast of Tenerife [8,84]. The massive landslide(s) directly facing the neighboring island of Gran Canaria must have generated large waves travelling directly towards that target area. However, this relationship is not supported by the new 160–180 ka age interval provided by AAR analyses in *Glycymeris* (Table 1).

The age of the Güímar landslide has been estimated at ~830 ka, or somewhat older, as the first lava flow filling the landslide depression has been dated to around 1 Ma ([52] and references therein), which is consistent with the lower limit imposed by the 1.75 Ma age of the lavas underlying the tsunami deposits. On the other hand, the stratigraphic evidence for three different tsunamis events in Agaete would point to the occurrence of several time-differentiated landslides in the area of Güímar, a hypothesis previously proposed by [83], based on morphological features of the landslide scars (tsunami deposits from prehistoric megalandslides with layers deposited by multiple tsunamis have also been described in the Hawaiian islands [6,85]). Neither the AAR nor TL ages obtained in this study for the marine conglomerates agree with the postulated age for Güímar at around 0.83–1 Ma [83]. In this respect, it should be noted that the age determinations here

presented correspond to the two younger tsunami deposits located at the lowest elevations (50 to 80 m a.s.l.), at La Aldea and Llanos de Turman sites. The deposits at higher elevations in the Agaete valley, up to almost 200 m, may have an older age, corresponding to the older tsunami exposed at La Ruina or to other tsunami events.

The existing ages for both the landslides and tsunami deposits in the Canary islands, preclude a consistent relationship between specific landslides and tsunami deposits to be established, except for Teno and Isla Baja, although these phenomena can be constrained to a broad time-interval corresponding to the middle Pleistocene (~800 ka to ~160 ka ago).

7. Conclusions

The main results obtained from the geological, geomorphological, paleontological, and geochronological investigations carried out on the tsunami deposits identified in Tenerife, Gran Canaria, and Lanzarote, as well as their possible source areas and frequency, are summarized below.

1. Fossiliferous marine deposits composed of chaotic conglomerates have been identified and described in detail at several sites in Tenerife (Teno and Isla Baja), Gran Canaria (Agaete), and Lanzarote (Piedra Alta). In all of them, common sedimentological, geomorphological, and paleontological features unequivocally indicate a tsunamigenic origin.
2. According to the age determinations and stratigraphic relations of the investigated deposits, at least four to five tsunami events (or up to six if we consider the two successive tsunamis in Icod as individual events) have occurred, some of them presenting several inundation pulses.
3. A total of 144 age determinations were carried out, of which 105 correspond to amino acid racemization (AAR) analysis, 35 to U-series dating in corals, and four to the thermoluminescence (TL) technique. The overall results show that the tsunami deposits were emplaced during the middle Pleistocene, with an age younger than 168 ka for Teno and Isla Baja, between 140 and 200 ka in Agaete, and within the 154–221 ka age interval at Piedra Alta.
4. The maximum tsunami run-up heights associated with these deposits have been calculated according to their present elevation, estimated ages, and the coeval sea level position. Maximum tsunami wave run-ups of 180 and 270 m for Teno and Isla Baja, respectively, 290 m for Agaete, and 125 m for Piedra Alta are proposed.
5. The megatsunami waves are attributed to large flank landslides of the Canaries volcanic edifices. Attempts were made to establish relationships between the tsunami deposits and potential source landslides, based on their estimated ages and spatial distribution. The age for Teno and Isla Baja tsunami deposits (<168 ka), is in the same range of the Icod flank landslide and ensuing explosive eruption (165–175 ka), showing a strong correlation between the landslide/volcanic event and the tsunami inundations of the north shore of Tenerife. This is also supported by the specific lithological and sedimentological characteristics of the deposits.
6. The available geochronological data for the Agaete and Piedra Alta tsunami deposits precludes the establishment of reliable bi-univocal correlations with the potential landslide sources. In the case of Agaete, ages younger than 1.75 Ma (based on the age of underlying lavas), or between 160 and 180 ka according with AAR and TL results, have been proposed. These results prevent a possible relation with the admitted age for a single landslide at Güímar (at around 830 ka or older). However, the presence of at least three different tsunamis deposits in Agaete suggests that more recent landslides may have been generated within the Güímar valley.
7. Paleontological and biogeographical markers for Piedra Alta deposits suggest an age range for their emplacement between ~400 and ~500 ka, which is compatible with the age interval for landslides at La Orotava valley (~500 to 560 ka). However, AAR ages in the 154 to 221 ka range, do not preclude a correlation with the Icod event.

8. According to the global age results for the deposits, the main sources for tsunamis in the Canary Islands during the last 1 million years may have been megalandslides that affected the flanks of volcanic edifice of Tenerife, where, at least, seven large events have occurred in this period: one in the Icod valley, three at La Orotava, two in Güímar, and one in Micheque.
9. Considering the frequency of megalandslides during the last 1 million years in the Canaries, with possibly several overlapping landslides on the same island flank, it can be stated that correlative tsunami events have also occurred with a relatively high frequency during the Middle Pleistocene in the archipelago, with an average interval of 80 ka.

Supplementary Materials: Tables including the results of the age determination methods applied in this study are available online at https://www.mdpi.com/article/10.3390/geohazards2030013/s1.

Author Contributions: M.F., L.G.d.V., J.M. (José Madeira), C.A., J.C.G.-D., M.d.C.F., J.M. (Joaquín Meco) and J.F.B. contributed to the field survey, description and mapping of tsunami deposits, and sample collections. T.T. and J.E.O. performed AAR lab analyses, preparation of the samples, and verification and interpretation of the results. All authors contributed to the writing—original draft preparation; M.F., J.M. (José Madeira), C.A. contributed to the writing—review and editing. All authors have read and agreed to the published version of the manuscript.

Funding: This research was carried out with financial support from the Ministry of Science of Spain (CICYT—project GRANDETEN II n° CGL2008-01423) and the Geological Survey of Spain (IGME).

Institutional Review Board Statement: Not applicable.

Informed Consent Statement: Not applicable.

Data Availability Statement: The data presented in this study are available in this article and the Supplementary Data.

Acknowledgments: The authors would like to thank all the participants in the GRANDETEN II research project. We also thank M. Stein from the Geological Survey of Israel and S. Giralt from the Institute of Earth Sciences Jaume Almera (CSIC) for the U-Th analysis of coral fragments; and A. Millán and P.Beneitez from the Laboratorio de Datación y Radioquímica of the Universidad Autónoma de Madrid for the TL analysis of calcareous sediments. J.M. (José Madeira), C.A. and M.C.F. acknowledge the UIDB/50019/2020 project to IDL. We wish to thank the three anonymous reviewers for their encouraging comments and suggestions, which have indeed improved the manuscript.

Conflicts of Interest: The authors declare no conflict of interest.

References

1. Pararas-Carayannis, G. Analysis of mechanism of tsunami generation in Lituya Bay. *Sci. Tsunami Haz.* **1999**, *17*, 193–206.
2. Smith, D.E.; Shi, S.; Cullingford, R.A.; Dawson, A.G.; Firth, C.R.; Foster, I.D.L.; Fretwell, P.T.; Haggart, B.A.; Holloway, L.K.; Long, D. The Holocene Storegga slide tsunami in the United Kingdom. *Quat. Sci. Rev.* **2004**, *23*, 2291–2321. [CrossRef]
3. Bondevik, S.; Mangerud, J.; Dawson, S.; Dawson, A.; Lohneb, Ø. Evidence for three North Sea tsunamis at the Shetland Islands between 8000 and 1500 years ago. *Quat. Sci. Rev.* **2005**, *24*, 1757–1775. [CrossRef]
4. Moore, J.G.; Moore, G.W. Deposit from a giant wave on the Island of Lanai, Hawaii. *Science* **1984**, *226*, 1312–1315. [CrossRef] [PubMed]
5. Moore, G.W.; Moore, J.G. Large-scale bedforms in boulder gravel produced by giant waves in Hawaii. *GSA Spec. Papers* **1988**, *229*, 101–110.
6. Felton, E.A.; Crook, K.A.W.; Keating, B.H. The Hulopoe gravel, Lanai, Hawaii: New sedimentological data and their bearing on the "giant wave" (mega-tsunami) emplacement hypothesis. *Pure Appl. Geophys.* **2000**, *157*, 1257–1284. [CrossRef]
7. McMurtry, G.M.; Fryer, G.J.; Tappin, D.R.; Wilkinson, I.P.; Williams, M.; Fietzke, J.; Garbe-Schoenberg, D.; Watts, P. Megatsunami deposits on Kohala volcano, Hawaii, from flank collapse of Mauna Loa. *Geology* **2004**, *32*, 741–744. [CrossRef]
8. Pérez Torrado, F.J.; Paris, R.; Cabrera, M.C.; Schneider, J.L.; Wassmer, P.; Carracedo, J.C.; Rodriguez Santana, A.; Santana, F. Tsunami deposits related to flank collapse in oceanic volcanoes: The Agaete valley evidence, Gran Canaria, Canary Islands. *Mar. Geol.* **2006**, *227*, 135–149. [CrossRef]
9. Madeira, J.; Ferrer, M.; González de Vallejo, L.; Andrade, C.; Freitas, M.C.; Lomoschitz, A.; Hoffmann, D.L. Agaete revisited: New data on the Gran Canaria tsunamiites. *Geophys. Res. Abs.* **2011**, *13*, 2292-2.

10. Ferrer, M.; González de Vallejo, L.; Seisdedos, J.; Coello, J.J.; García, J.C.; Hernández, L.E.; Casillas, R.; Martín, C.; Rodríguez, J.A.; Madeira, J.; et al. Güímar and La Orotava megalandslides (Tenerife) and tsunami deposits in Canary islands. In *Landslide Science and Practise: Complex Environment*; Margottini, C., Canuti, P., Sassa, K., Eds.; Springer: Berlin/Heidelberg, Germany, 2013; Volume 5, pp. 27–33. [CrossRef]
11. Paris, R.; Bravo, J.J.C.; Martín-González, E.; Kelfoun, K.; Nauret, F. Explosive eruption, flank collapse and megatsunami at Tenerife ca. 170 ka. *Nat. Commun.* **2017**, *8*, 15246. [CrossRef]
12. Paris, R.; Giachetti, T.; Chevalier, J.; Guillou, H.; Frank, N. Tsunami deposits in Santiago Island (Cape Verde archipelago) as possible evidence of a massive flank failure of Fogos volcano. *Sediment. Geol.* **2011**, *239*, 129–145. [CrossRef]
13. Madeira, J.; Ramalho, R.S.; Mata, J.; Moreira, M.; Hoffmann, D. A geological record of multiple Pleistocene tsunami inundations in an oceanic island: The case of Maio, Cape Verde. *Sedimentology* **2020**, *67*, 1529–1552. [CrossRef]
14. Ramalho, R.S.; Winckler, G.; Madeira, J.; Helffrich, G.R.; Hipólito, A.R.; Quartau, R.; Adena, K.; Schaefer, J.M. Hazard potential of volcanic flank collapses raised by new megatsunami evidence. *Sci. Adv.* **2015**, *1*, e1500456. [CrossRef] [PubMed]
15. Bryant, E. *Tsunami: The Underrated Hazard*, 2nd ed.; Springer: Berlín, Germany, 2008; p. 330.
16. Pararas-Carayannis, G. The tsunami generated from the eruption of the volcano of Santorini in the Bronze Age. *Sci. Tsunami Haz.* **1988**, *6*, 23–30.
17. Carey, S.; Morelli, D.; Sigurdsson, H.; Bronto, S. Tsunami deposits from major explosive eruptions: An example from the 1883 eruption of Krakatau. *Geology* **2001**, *29*, 347–350. [CrossRef]
18. Smit, J.; Roep, T.B.; Alvarez, W.; Montanari, A.; Claeys, P.; Grajales-Nishimura, J.M.; Bermudez, J. Coarse-grained, clastic sandstone complex at the K/T boundary around the Gulf of Mexico: Deposition by tsunami waves induced by the Chicxulub impact? In *The Cretaceous-Tertiary Event and Other Catastrophes in Earth History*; Ryder, G., Fastovsky, D., Gartner, S., Eds.; Special Paper 307; Geological Society of America: Boulder, CO, USA, 1996; pp. 151–182.
19. Bourgeois, J.; Hansen, T.A.; Wiberg, P.L.; Kauffman, E.G. A tsunami deposit at the Cretaceous-Tertiary boundary in Texas. *Science* **1998**, *241*, 567–570. [CrossRef]
20. Whelan, F.; Kelletat, D. Submarine slides on volcanic islands—A source for mega-tsunamis in the Quaternary. *Prog. Phys. Geog.* **2003**, *27*, 198–216. [CrossRef]
21. Keating, B.H.; McGuire, W.J. Island edifice failures and associated tsunami hazards. *Pure Appl. Geophys.* **2000**, *157*, 899–955. [CrossRef]
22. McMurtry, G.M.; Watts, P.; Fryer, G.J.; Smith, J.R.; Imamura, F. Giant landslides, mega-tsunamis, and paleo-sea level in the Hawaiian Islands. *Mar. Geol.* **2004**, *203*, 219–233. [CrossRef]
23. Moore, J.G.; Clague, D.A.; Holcomb, R.T.; Lipman, P.W.; Normark, W.R.; Torresan, M.E. Prodigious submarine landslides on the Hawaiian Ridge. *J. Geophys. Res.* **1989**, *94*, 17465–17484. [CrossRef]
24. Watts, A.B.; Masson, D.G. A giant landslide on the north flank of Tenerife, Canary Islands. *J. Geophys. Res.* **1995**, *100*, 24487–24498. [CrossRef]
25. Teide Group. Morphometric interpretation of the northwest and southeast slopes of Tenerife, Canary Islands. *J. Geophys. Res.* **1997**, *102*, 20325–20342. [CrossRef]
26. Moore, J.G.; Bryan, W.B.; Ludwig, K.R. Chaotic deposition by a giant wave, Molokai, Hawaii. *Geol. Soc. Am. Bull.* **1994**, *106*, 962–967. [CrossRef]
27. Moore, A.L. Landward fining in onshore gravel as evidence for a late Pleistocene tsunami on Molokai, Hawaii. *Geology* **2000**, *28*, 247–250. [CrossRef]
28. Oehler, J.F.; Lénat, J.F.; Labazuy, P. Growth and collapse of the Reunion Island volcanoes. *Bull. Volcanol.* **2008**, *70*, 717–742. [CrossRef]
29. Tibaldi, A. Multiple sector collapses at Stromboli volcano, Italy: How they work. *Bull. Volcanol.* **2001**, *63*, 112–125. [CrossRef]
30. Tanner, L.H.; Calvari, S. Unusual sedimentary deposits on the SE side of Stromboli volcano, Italy: Products of a tsunami caused by the ca. 5000 years BP Sciara del Fuoco collapse? *J. Volcanol. Geotherm. Res.* **2004**, *137*, 329–340. [CrossRef]
31. Watt, S.F.L.; Karstens, J.; Berndt, C. Volcanic-island lateral collapses and their submarine deposits. In *Volcanic Debris Avalanches. Advances in Volcanology*; Roverato, M., Dufresne, A., Procter, J., Eds.; Springer: Cham, Switzerland, 2021; pp. 255–279. [CrossRef]
32. Karstens, J.; Berndt, C.; Urlaub, M.; Watt, S.F.L.; Micallef, A.; Ray, M.; Klaucke, I.; Muff, S.; Klaeschen, D.; Kühn, M.; et al. From gradual spreading to catastrophic collapse—Reconstruction of the 1888 Ritter Island volcanic sector collapse from high-resolution 3D seismic data. *Earth Planet. Sci. Lett.* **2019**, *517*, 1–13. [CrossRef]
33. Ward, S.N.; Day, S. Ritter Island Volcano-lateral collapse and the tsunami of 1888. *Geophys. J. Int.* **2003**, *154*, 891–902. [CrossRef]
34. Day, S.; Llanes, P.; Silver, E.; Hoffmann, G.; Ward, S.; Driscoll, N. Submarine landslide deposits of the historical lateral collapse of Ritter Island, Papua New Guinea. *Mar. Pet. Geol.* **2015**, *67*, 419–438. [CrossRef]
35. Satake, K. Volcanic origin of the 1741 Oshima-Oshima tsunami in the Japan Sea. *Earth Planets Space* **2007**, *59*, 381–390. [CrossRef]
36. Sassa, K.; Dang, K.; Yanagisawa, H.; He, B. A new landslide-induced tsunami simulation model and its application to the 1792 Unzen-Mayuyama landslide-and-tsunami disaster. *Landslides* **2016**, *13*, 1405–1419. [CrossRef]
37. Wang, J.; Ward, S.N.; Xiao, L. Tsunami Squares modeling of landslide generated impulsive waves and its application to the 1792 Unzen-Mayuyama mega-slide in Japan. *Eng. Geol.* **2019**, *256*, 121–137. [CrossRef]
38. Tsuji, Y.; Hino, T. Damage and inundation height of the 1792 Shimabara landslide tsunami along the coast of Kumamoto Prefecture. *Bull. Earthq. Res. Inst. Univ. Tokyo* **1993**, *68*, 91–176, (In Japanese with English abstract).

39. Akagi, Y. The tsunami height and damaged area of Tsunami occurred in 1792 in Shimabara Peninsula. *Hist. Geogr.* **2001**, *43*, 4–19. (In Japanese)
40. Harris, R.; Major, J. Waves of destruction in the East Indies: The Wichmann catalogue of earthquakes and tsunami in the Indonesian region from 1538 to 1877. In *Geohazards in Indonesia: Earth Science for Disaster Risk Reduction*; Cummins, P.R., Meilano, I., Eds.; Special Publication 441; The Geological Society of London: London, UK, 2017. [CrossRef]
41. Grilli, S.T.; Tappin, D.R.; Carey, S.; Watt, S.F.L.; Ward, S.N.; Grilli, A.R.; Engwell, S.L.; Zhang, C.; Kirby, J.T.; Schambach, L.; et al. Modelling of the tsunami from the December 22, 2018 lateral collapse of Anak Krakatau volcano in the Sunda Straits, Indonesia. *Sci. Rep.* **2019**, *9*, 11946. [CrossRef]
42. Satake, K.; Kato, Y. The 1741 Oshima-Oshima eruption: Extent and volume of submarine debris avalanche. *Geophys. Res. Lett.* **2001**, *28*, 427–430. [CrossRef]
43. Watt, S.F.L.; Karstens, J.; Micallef, A.; Berndt, C.; Urlaub, M.; Ray, M.; Desai, A.; Sammartini, M.; Klaucke, I.; Böttner, C.; et al. From catastrophic collapse to multi-phase deposition: Flow transformation, seafloor interaction and triggered eruption following a volcanic-island landslide. *Earth Planet. Sci. Lett.* **2019**, *517*, 135–147. [CrossRef]
44. Krastel, S.; Schmincke, H.-U.; Jacobs, C.L.; Rihm, R.; Le Bas, T.P.; Alibés, B. Submarine landslides around the Canary Islands. *J. Geophys. Res.* **2001**, *106*, 3977–3997. [CrossRef]
45. Masson, D.G.; Watts, A.B.; Gee, M.J.R.; Urgeles, R.; Mitchell, N.C.; Le Bas, T.P.; Canals, M. Slope failures on the flanks of the western Canary Islands. *Earth-Sci. Rev.* **2002**, *57*, 1–35. [CrossRef]
46. Cantagrel, J.M.; Arnaud, N.O.; Ancochea, E.; Fuster, J.M.; Huertas, M.J. Repeated debris avalanches on Tenerife and genesis of Las Cañadas caldera wall (Canary Islands). *Geology* **1999**, *27*, 739–742. [CrossRef]
47. Boulesteix, T.; Hildenbrand, A.; Soler, V.; Quidelleur, X.; Gillot, P.Y. Coeval giant landslides in the Canary Islands: Implications for global, regional and local triggers of giant flank collapses on oceanic volcanoes. *J. Volcanol. Geotherm. Res.* **2013**, *257*, 90–98. [CrossRef]
48. Urgeles, R.; Masson, D.G.; Canals, M.; Watts, A.B.; Le Bas, T. Recurrent large-scale landsliding on the west flank of La Palma, Canary Islands. *J. Geophys. Res. Atmos.* **1999**, *1042*, 25331–25348. [CrossRef]
49. Carracedo, J.C.; Day, S.J.; Guillou, H.; Pérez Torrado, F.J. Giant Quaternary landslides in the evolution of La Palma and El Hierro, Canary Islands. *J. Volcanol. Geotherm. Res.* **1999**, *94*, 169–190. [CrossRef]
50. Urgeles, R.; Canals, M.; Masson, D.G. Flank stability and processes off the western Canary Islands: A review from El Hierro and La Palma. *Sci. Mar.* **2001**, *65* (Suppl. 1), 21–31. [CrossRef]
51. León, R.; Somoza, L.; Urgeles, R.; Medialdea, T.; Ferrer, M.; Biain, A.; García-Crespo, J.; Mediato, J.F.; Galindo, I.; Yepes, J.; et al. Multi-event oceanic island landslides: New onshore-offshore insights from El Hierro Island, Canary Archipelago. *Mar. Geol.* **2017**, *393*, 156–175. [CrossRef]
52. Ferrer, M.; González de Vallejo, L.I.; García, J.C. Geochronology of the megalandslides of the last million years in Tenerife. Part I: A review and new Ar/Ar ages. *Bol. Inst. Geol. Min. Esp.* **2020**, *131*, 903–940, (In Spanish with abridget English version).
53. Meco, J.; Ballester, J.; Betancort, J.F.; Cilleros, A.; Scaillet, S.; Guillou, H.; Carracedo, J.C.; Lomoschitz, A.; Petit-Maire, N.; Ramos, A.J.G.; et al. *Historia Geológica del Clima en Canarias*; Meco, J., Ed.; Laboratorio de Paleontología: Las Palmas, Spain, 2008; p. 296. ISBN 978-84-691-5551-6. Available online: http://acceda.ulpgc.es/bitstream/10553/700/1/4339.pdf (accessed on 14 April 2021).
54. Criado, C.; Yanes, A. Acerca de las paleoformas marinas cuaternarias de Teno Bajo (Tenerife, I. Canarias). In *Geomorfología Litoral y Quaternari. Homenaje al Profesor V.M. Roselló i Verger*; Santjaume, E., Mateu, J.F., Eds.; Universidad de Valencia: Valencia, Spain, 2005; pp. 113–122.
55. Ferrer, M.; Seisdedos, J.; González de Vallejo, L.I. The role of hyaloclastite rocks in the stability of the volcanic island flanks of Tenerife. In *Volcanic Rock Mechanics*; Olalla, C., Hernandez, L.E., Rodriguez-Losada, J.A., Perucho, A., González-Gallego, J., Eds.; CRC Press/Balkema: Boca Raton, FL, USA, 2010; pp. 167–170. ISBN 978-0-415-58478-4.
56. Seisdedos, J.; Ferrer, M.; González de Vallejo, L.I. Geological and geomechanical models of the pre-landslide volcanic edifice of Güímar and La Orotava mega-landslides (Tenerife). *J. Volcanol. Geotherm. Res.* **2012**, *239–240*, 92–110. [CrossRef]
57. Ferrer, M.; González de Vallejo, L.I.; González, S.; Jiménez, E. Stability and failure mechanisms of large landslides in the volcanic island flanks of the Canary Islands. In *Engineering Geology for Society and Territory*; Lollino, G., Manconi, A., Clague, J., Shan, W., Chiarle, M., Eds.; Springer Int. Pub.: Cham, Switzerland, 2015; Volume 2, pp. 915–919. ISBN 978-3-319-09056-6. [CrossRef]
58. Andrade, C.; Freitas, M.C.; Madeira, J. *Report of the Visit to Gran Canaria to Assess the Origin of the Agaete Chaotic Marine Conglomerates*; Project GRANDETEN-II (CGL2008-01423); Centro de Documentación IGME: Madrid, Spain, 2010; p. 11, Unpublished report.
59. Madeira, J.; Andrade, C.; Freitas, M.C. *Report of the Visit to Tenerife to Assess the Origin of the Chaotic Marine Breccias of Teno-Buenavista Region*; Project GRANDETEN II (CGL2008-01423); Centro de Documentación IGME: Madrid, Spain, 2011; p. 10, Unpublished report.
60. Paris, R.; Ramalho, R.S.; Madeira, J.; Ávila, S.; May, S.M.; Rixhon, G.; Engel, M.; Brückner, H.; Herzog, M.; Schukraft, G.; et al. Mega-tsunami conglomerates and flank collapses of ocean island volcanoes. *Mar. Geol.* **2018**, *395*, 168–187. [CrossRef]
61. Costa, P.J.; Dawson, S.; Ramalho, R.S.; Engel, M.; Dourado, F.; Bosnic, I.; Andrade, C. A review on onshore tsunami deposits along the Atlantic coasts. *Earth-Sci. Rev.* **2021**, *212*, 103441. [CrossRef]
62. Kaufman, D.S.; Manley, W.F. A new procedure for determining dl amino acid ratios in fossils using reverse phase liquid chromatography. *Quat. Sci. Rev.* **1998**, *17*, 987–1000. [CrossRef]

63. Zazo, C.; Goy, L.L.; Dabrio, C.; Bardají, T.; Hillaire-Marcel, C.; Ghaleb, B.; González-Delgado, J.A.; Soler, V. Pleistocene raised marine terraces of the Spanish Mediterranean and Atlantic coasts: Records of coastal uplift, sea-level highstands and climate changes. *Mar. Geol.* **2003**, *194*, 103–133. [CrossRef]
64. Zazo, C.; Goy, J.L.; Hillaire-Marcel, C.; Gillot, P.Y.; Soler, V.; González, J.Á.; Dabrio, C.J.; Ghaleb, B. Raised marine sequences of Lanzarote and Fuerteventura revisited-a reappraisal of relative sea-level changes and vertical movements in the eastern Canary Islands during the Quaternary. *Quat. Sci. Rev.* **2002**, *21*, 2019–2046. [CrossRef]
65. Clauzel, T.; Maréchal, C.; Fourel, F.; Barral, A.; Amiot, R.; Betancort, J.F.; Lomoschitz, A.; Meco, J.; Lécuyer, C. Reconstruction of sea-surface temperatures in the Canary Islands during Marine Isotope Stage 11. *Quat. Res.* **2019**, 1–15. [CrossRef]
66. Carracedo, J.; Badiola, E.R.; Guillou, H.; Paterne, M.; Scaillet, S.; Torrado, F.P.; Paris, R.; Fra-Paleo, U.; Hansen, A. Eruptive and structural history of Teide Volcano and rift zones of Tenerife, Canary Islands. *GSA Bull.* **2007**, *119*, 1027–1051. [CrossRef]
67. Stein, M. U-Th dating of coral fragments from the Canary islands, Spain. In *Preliminary Report. Geological Survey of Israel*; IGME: Madrid, Spain, 2013; Unpublished.
68. Stein, M. U-Th dating of coral fragments from the Canary islands, Spain. In *Report. Geological Survey of Israel*; IGME: Madrid, Spain, 2017; Unpublished.
69. Meco, J.; Stearn, C.E. Emergent littoral deposits in the Eastern Canary Islands. *Quat. Res.* **1981**, *15*, 199–208. [CrossRef]
70. Muhs, D.R.; Meco, J.; Simmons, K.R. Uranium-series ages of corals, sea level history, and palaeozoogeography, Canary Islands, Spain: An exploratory study for two Quaternary interglacial periods. *Palaeogeogr. Palaeoclim. Palaeoecol.* **2014**, *394*, 99–118. [CrossRef]
71. Meco, J.; Guillou, H.; Carracedo, J.-C.; Lomoschitz, A.; Ramos, A.G.; Rodríguez-Yánez, J.-J. The maximum warmings of the Pleistocene world climate recorded in the Canary Islands. *Palaeogeogr. Palaeoclim. Palaeoecol.* **2002**, *185*, 197–210. [CrossRef]
72. Bintanja, R.; Van De Wal, R.S.; Oerlemans, J. Modelled atmospheric temperatures and global sea levels over the past million years. *Nat. Cell Biol.* **2005**, *437*, 125–128. [CrossRef] [PubMed]
73. Dabrío, C.; Polo, M.D. Sea level changes. *Enseñanza de las Ciencias de la Tierra* **2015**, *23*, 171–179, (In Spanish with English Abstract).
74. Carracedo, J.-C. Growth, structure, instability and collapse of Canarian volcanoes and comparisons with Hawaiian volcanoes. *J. Volcanol. Geotherm. Res.* **1999**, *94*, 1–19. [CrossRef]
75. Kröchert, J.; Maurer, H.; Buchner, E. Fossil beaches as evidence for significant uplift of Tenerife, Canary Islands. *J. Afr. Earth Sci.* **2008**, *51*, 220–234. [CrossRef]
76. Carracedo, J.C.; Guillou, H.; Nomade, S.; Rodriguez-Badiola, E.; Pérez-Torrado, F.J.; González, A.R.; Paris, R.; Troll, V.R.; Wiesmaier, S.; Delcamp, A.; et al. Evolution of ocean-island rifts: The northeast rift zone of Tenerife, Canary Islands. *GSA Bull.* **2010**, *123*, 562–584. [CrossRef]
77. Guillou, H.; Carracedo, J.; Duncan, R. K–Ar, 40Ar–39Ar ages and magnetostratigraphy of Brunhes and Matuyama lava sequences from La Palma Island. *J. Volcanol. Geotherm. Res.* **2001**, *106*, 175–194. [CrossRef]
78. Quidelleur, X.; Hildenbrand, A.; Samper, A. Causal link between Quaternary paleoclimatic changes and volcanic islands evolution. *Geophys. Res. Lett.* **2008**, *35*, 5. [CrossRef]
79. Biain, A.; León, R.; Urgeles, R.; Somoza, L.; Medialdea, T.; Ferrer, M.; González, F.J. Onshore and offshore geomorphological features of the El Golfo debris avalanche (El Hierro, Canary islands). In *Submarine Mass Movements and Their Consequences. Advances in Natural and Technological Hazards Research*; Lamarche, G., Mountjoy, J., Bull, S., Hubble, T., Krastel, S., Lane, E., Micallef, A., Moscardelli, L., Mueller, C., Pecher, I., et al., Eds.; Springer: Cham, Switzerland, 2015; pp. 83–92. [CrossRef]
80. Longpré, M.A.; Chadwick, J.P.; Wijbrans, J.; Iping, R. Age of the El Golfo debris avalanche, El Hierro (Canary Islands): New constraints from laser and furnace 40Ar/39Ar dating. *J. Volcanol. Geotherm. Res.* **2011**, *203*, 76–80. [CrossRef]
81. Huertas, M.J.; Arnaud, N.O.; Ancochea, E.; Cantagrel, J.M.; Fuster, J.M. $^{40}Ar/^{39}Ar$ stratigraphy of pyroclastic units from the Cañadas Volcanic Edifice (Tenerife, Canary Islands) and their bearing on the structural evolution. *J. Volcanol. Geotherm. Res.* **2002**, *115*, 351–365. [CrossRef]
82. Boulesteix, T.; Hildenbrand, A.; Gillot, P.Y.; Soler, V. Eruptive response of oceanic islands to giant landslides: New insights from the geomorphologic evolution of the Teide-Pico Viejo volcanic complex (Tenerife, Canary). *Geomorphology* **2012**, *138*, 61–73. [CrossRef]
83. Ferrer, M.; González de Vallejo, L.I.; García, J.C. Geochronology of the megalandslides of the last million years in Tenerife. Part II: New contributions to knowledge about the landslides. *Bol. Inst. Geol. Min. Esp.* **2020**, *131*, 941–970, (In Spanish with abridget English version).
84. Giachetti, T.; Paris, R.; Kelfoun, K.; Torrado, F.J.P. Numerical modelling of the tsunami triggered by the Güìmar debris avalanche, Tenerife (Canary Islands): Comparison with field-based data. *Mar. Geol.* **2011**, *284*, 189–202. [CrossRef]
85. Rubin, K.H.; Fletcher, C.H.; Sherman, C. Fossiliferous Lana'i deposits formed by multiple events rather than a single giant tsunami. *Nat. Cell Biol.* **2000**, *408*, 675–681. [CrossRef] [PubMed]